# Spreading Factor Optimization and Random Access Stability Control for IMT-2000

HO Chi-Fong

A Thesis Submitted in Partial Fulfillment
of the Requirements for the Degree of
Master of Philosophy
in
Information Engineering


August 2000

# Acknowledgement

I would like to express my deepest gratitude to my thesis supervisor Professor Tak-Shing Peter Yum for his continuous support, intelligent guidance, encouragement and numerous patient revisions for my thesis throughout this research work. His valuable comments and suggestions have a fundamental influence on the development of this thesis. Actually, every discussion with him brought me thought-provoking insights.

My special thanks are to my colleagues and friends, Yin-Man Lee, Ho-Yuet Kwan and Xiao-Wei Ding, for their contributions to this thesis, as well as for all conversations we shared.

I am thankful to my family and all my friends here at CUHK and elsewhere around the world, for their continuous support. Finally, I thank my teachers, past and present, for without their guidance, I would not be here today.

# Abstract

One primary focus of today's wireless networking technology is on the efficient integration of multimedia traffic such as voice, data and video. However, the second generation wireless communication systems are limited in the maximum supported data rate. For the third generation wireless communication more advanced services supported.

Third generation mobile communication services will roll out in 2002. This new standard supports higher data rate services than that in 2G and 2.5G systems. There are five 3G radio standards. Hence, there are many interested problems in it, such as resources allocation, power control, mobility management, data packet routing, and finding the system throughput. In this thesis, we work on the UTRA standard. We first introduce the physical layer of the IMT-2000 UTRA in Chapter 1. We then purpose a FDD downlink Spreading Factor Assignment Algorithm with minimized bandwidth wastage in Chapter 2. This algorithm is simple, easy to implement. Moreover, it can lower the average wastage from 26% to 10%.

In Chapter 3, we study a Slotted Aloha type random access model based on the UTRA TD/CDMA standard. First, we find the collision probability and the throughput by mathematical analysis. Then, we purposed a stability control

algorithm. It can maintain system stability with a near maximum throughput under a very high arrival rate of single class random access bursts. Moreover, We also study the Random Access Channel Stability Control Algorithm for multi-class random access burst traffic. Since, exact analysis of this model is mathematically intractable, computer simulation is used. Simulation results show that the system is always stable with the use of our algorithm.

# 摘 要

當前，無線通訊網絡技術的一個主要課題是如何有效地集成諸如語音、數據、圖像等多媒體數據。 但是第二代無線通訊系統支持的最高數據速率有限。 第三代無線通訊在語音和低速數據之外，能夠提供比當今無線通訊系統更先進的服務。

第三代移動無線通訊服務將在 2002 年推出。 這個新的標準支持比第二和第二點五代系統更高的數據速率， 其空中接口是一個全新的標準。 因此， 這個標準存在很多有趣的新問題， 比如信道分配和系統通過率。 在本文中， 我們研究了 UTRA 的標準， 首先提出了一種基於 FDD 的下行信道擴頻因子分配算法， 本算法簡單， 易於實現，它有效地將帶寬的利用率從 74%提高到 90%。

在第三章中，我們研究了一種基於UTRA TD/CDMA 標準的隨機接入模型。首先， 我們用數學分析的方法計算出碰撞概率和通過率；然後， 本文提出一種穩定的控制算法。 它能在保証對於極高速率的突發性隨機接入數據有幾乎最高通過率的同時， 維持了系統的穩定性。 由於對這個模型進行精確數學分析是不可行的， 我們採用了計算機仿真的方法來進行研究；最後本文研究了用於多種類型突發性隨機接入數據的隨機接入信道穩定控制算法。 仿真的結果表明這個算法能保証系統始終穩定。

# List of Abbreviations

| | |
|---|---|
| ARQ | Automatic Repeat Request |
| BCCH | Broadcast Control Channel |
| BCH | Broadcast Channel |
| BER | Bit Error Rate |
| BPSK | Binary Phase Shift Keying |
| BS | Base Station |
| BSC | Base Station Controller |
| CA | Capacity Allocation |
| CBR | Constant Bit Rate |
| CCCH | Common Control Channel |
| CCH | Control Channel |
| CCPCH | Common Control Physical Channel |
| CDMA | Code Division Multiple Access |
| CN | Core Network |
| CPICH | Common Pilot Channel |
| CPCH | Common Packet Channel |
| CRC | Cyclic Redundancy Check |
| CRNC | Controlling Radio Network Controller |
| CS | Circuit Switched |
| CTCH | Common Traffic Channel |
| CTDMA | Code Time Division Multiple Access |
| DC | Dedicated Control (SAP) |

| | |
|---|---|
| DCA | Dynamic Channel Allocation |
| DCCH | Dedicated Control Channel |
| DCH | Dedicated Channel |
| DL | Downlink (Forward Link) |
| DPCCH | Dedicated Physical Control Channel |
| DPCH | Dedicated Physical Channel |
| DPDCH | Dedicated Physical Data Channel |
| DSCH | Downlink Shared Channel |
| DTCH | Dedicated Traffic Channel |
| FACH | Forward Access Channel |
| FDD | Frequency Division Duplex |
| FDMA | Frequency Division Multiple Access |
| FEC | Forward Error Correction |
| GMSK | Gaussian Minimum Shift Keying |
| GPRS | General Packet Radio System |
| GSM | Global System for Mobile communications |
| GTP | GPRS Tunneling Protocol |
| HO | Handover |
| IMSI | International Mobile Subscriber Identity |
| IP | Internet Protocol |
| ITU | International Telecommunication Union |
| L1 | Layer 1 (physical layer) |
| L2 | Layer 2 (data link layer) |
| L3 | Layer 3 (network layer) |

| | |
|---|---|
| LAC | Link Access Control |
| LLC | Logical Link Control |
| MA | Multiple Access |
| MAC | Medium Access Control |
| Mcps | Mega-chips per second |
| MM | Mobility Management |
| MNC | Mobile Network Code |
| MS | Mobile Station |
| MSID | Mobile Station Identifier |
| MUI | Mobile User Identifier |
| NRT | Non-Real Time |
| O&M | Operation and Management |
| OVSF | Orthogonal Variable Spreading Factor |
| PCPCH | Physical Common Packet Channel |
| PCCPCH | Primary Common Control Physical Channel |
| PCS | Personal Communication System |
| PDSCH | Physical Downlink Shared Channel |
| PDU | Protocol Data Unit |
| PHY | Physical layer |
| PI | Page Indicator |
| PICH | Page Indication Channel |
| PID | Packet Identification |
| PLMN | Public Land Mobile Network |
| PRACH | Physical Random Access Channel |
| PS | Packet Switched |

| | |
|---|---|
| PSCH | Physical Shared Channel |
| QoS | Quality of Service |
| QPSK | Quadrature (Quaternary) Phase Shift Keying |
| RAB | Radio Access Bearer |
| RACH | Random Access Channel |
| RANAP | Radio Access Network Application Part |
| RF | Radio Frequency |
| RL | Radio Link |
| RLC | Radio Link Control |
| RNC | Radio Network Controller |
| RNTI | Radio Network Temporary Identity |
| RRM | Radio Resource Management |
| RT | Real Time |
| RU | Resource Unit |
| SAP | Service Access Point |
| SCCH | Synchronization Control Channel |
| SCCPCH | Secondary Common Control Physical Channel |
| SCH | Synchronization Channel |
| SDU | Service Data Unit |
| SF | Spreading Factor |
| SFN | System Frame Number |
| SIR | Signal-to-Interference Ratio |
| SMS | Short Message Service |
| SP | Switching Point |

| | |
|---|---|
| SRNC | Serving Radio Network Controller |
| SRNS | Serving RNS |
| SS7 | Signaling System No. 7 |
| TCH | Traffic Channel |
| TDD | Time Division Duplex |
| TDMA | Time Division Multiple Access |
| TF | Transport Format |
| TFC | Transport Format Combination |
| TFCI | Transport Format Combination Indicator |
| TFCS | Transport Format Combination Set |
| TFI | Transport Format Indicator |
| TFS | Transport Format Set |
| TMSI | Temporary Mobile Subscriber Identity |
| TPC | Transmit Power Control |
| TrCH | Transport Channel |
| TTI | Transmission Timing Interval |
| TX | Transmit |
| UDP | User Datagram Protocol |
| UE | User Equipment |
| UL | Uplink (Reverse Link) |
| UMTS | Universal Mobile Telecommunications System |
| USCH | Uplink Shared Channel |
| UTRA | Universal Terrestrial Radio Access |
| UTRAN | Universal Terrestrial Radio Access Network |
| VBR | Variable Bit Rate |

# Contents

# Chapter 1

# Introduction

## 1.1 Introduction

Mobile communications experienced enormous growth during the last twenty years. First-generation mobile systems such as AMPS, TACS, and NMT using analog modulation for voice services were introduced in the early '80s. Second-generation systems, which use digital modulation, were introduced in the later 1980s. Global System for Communications (GSM), Personal Digital Cellular (PDC), IS-136, and IS-95 are second-generation systems. The services offered by these systems cover speech and low-bit-rate data. The 2.5G systems isupgraded version of the 2G system, offer more advanced services such as medium-bit-rate (up to 100kbps) circuit- and packet-switched data. High-speed circuit-switched data service (HSCSD), General Packet Radio Service (GPRS), Enhanced Data Rates for GSM Evolution (EDGE), IS95A and IS95B are 2.5G systems.

The global standards body for communications is the International Telecommunications Union (ITU). The 3G standards effort is called International Mobile

Telephone 2000 (IMT-2000). 3G systems can offer at least 144 kbps (preferably 384kbps) for high-mobility users with wide-area coverage and 2Mbps for low-mobility users with the lack of spectrum motivate the development of more spectrum-efficient radio technologies.

IMT-2000 does not only work on radio technologies, but also on the networking infrastructure. It is building on backward compatibility to second-generation networks. One objective is to allow users to seamlessly roam from private networks (e.g. Ethernet, 802.11, 802.15) to public networks. Such roaming will require the implementation of standards such as Mobile IP. Data, voice and multimedia traffic, are split into packets and transmitted over the networks.

In this thesis, we first introduce some 2.5G systems and show the evolution paths from 2G to 3G. After that, we introduce the air interference of the UTRA, a 3G standard. The 3G physical layer is different from 2G and 2.5G systems. In Chapter 2, we also purpose a Spreading Factor Optimization Algorithm for UTRA FDD downlink dedicated channels. This algorithm can minimize the bandwidth wastage by fully utilizing the number of usable dedicated channels. In Chapter 3, we analysis the performance of TD/CDMA Slotted ALOHA type system. We find the system throughput and the system delay. Moreover, we propose a Random Access Channel Stability Control Algorithm for multi-class random access traffic and analyze it with computer simulations. In Chapter 4, we conclude the works in this thesis and list some interested problems of the UTRA system.

## 1.2 The 2.5G Systems

### 1.2.1 HSCSD

Traditional GSM Circuit Switched Data (operating at slow speeds of 9,600-14,400 bps) supports one user per channel per time slot. High Speed Circuit Switched Data (HSCSD) gives a single user simultaneous access to multiple channels (up to four) at the same time with a data rate up to 57.6 kbps. This is broadly equivalent to providing the same transmission rate as that available over one ISDN B-Channel. Some Mobile Switching Centres (MSCs) are limited to 64 kbps maximum throughput.

### 1.2.2 GPRS

The packet-switched data service for GSM is called General Packet Radio Service (GPRS). It can combine up to 8 (out of 8 available) time slots in each time interval for IP-based packet data speeds up to a maximum theoretical rate of 160 kbps. However, a typical GPRS device may not use all 8 time slots. GPRS supports both IP and X.25 networking. GPRS can be added to GSM infrastructures quite readily. It can work on the 200 kHz GSM radio channels and does not require new radio spectrum. The principal new infrastructure elements are called the Gateway GPRS Support Node (GGSN) and the Serving GPRS Support Node (SGSN). The GGSN provides the interconnection to other networks such as the Internet or private networks, while the SGSN tracks the location of mobile devices and routes packet traffic to them.

### 1.2.3 EDGE

The phase after GPRS is called Enhanced Data Rates for GSM Evolution (EDGE). EDGE introduces new methods at the physical layer including a new form of modulation (8 PSK) and different ways of encoding data to protect against errors. Meanwhile, higher layer protocols, such as those used by the GGSN and SGSN, stay the same. The result is that EDGE will deliver data rates up to 500 kbps using the same GPRS infrastructure. The 500 kbps bandwidth is shared by multiple users in each sector of a cell. So, practical throughputs may be only half the maximum rate.

### 1.2.4 IS-136

The Universal Wireless Communications Consortium (UWCC) embraces EDGE for IS-136 networks. Since the IS-136 networks use 30 kHz radio channels. Deploying EDGE will require new radios in base stations to support the 200 kHz data channels. The GGSN and SGSN will be virtually the same for both GSM and IS-136 networks. EDGE data users can roam between IS-136 and GSM networks.

## 1.3 The Evolution from 2G/2.5G to 3G

### 1.3.1 GSM Data Evolution

GSM Data Evolution is evolving in the following way:

The GSM data evolution path always requires new network infrastructure and new phones. Every one of the future GSM data services from HSCSD on

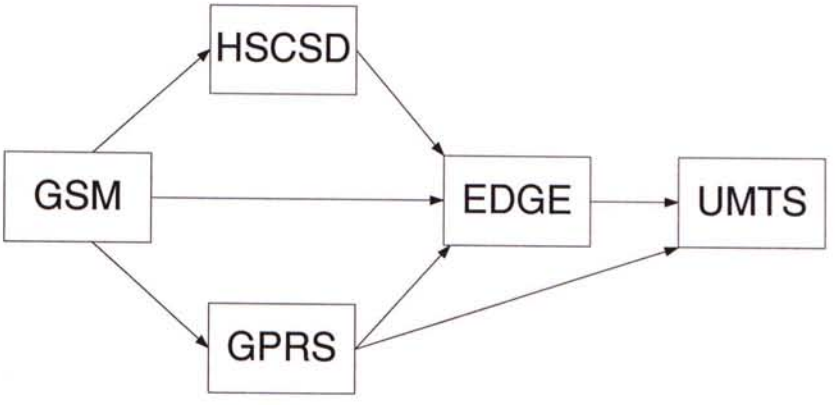


Figure 1.1: GSM Path to 3G

requires the purchase of a new mobile phone. HSCSD, WAP, GPRS, EDGE, and 3G require new handsets. 3G handsets will not work on EDGE or WCDMA base stations. However, multiband GSM/ 3G, GSM/ GPRS, GSM/ EDGE terminals will be available. On the infrastructure side, a GSM Network Operator must make new investments in base stations for GPRS, EDGE and 3G. Once the GPRS backbone is implemented, the evolution to 3G requires only evolution and enhancements on the air interface related equipment.

### 1.3.2 TDMA Data Evolution

TDMA is also known as D-AMPS (Digital Advanced Mobile Phone System) and is defined in the ANSI-136 standard.

Both TDMA and CDMA use an intersystem signaling protocol known as IS-41. GSM has GSM 03.40 for the transport layer and GSM 09.02 for the MAP layer. In TDMA, the teleservice layer is defined as part of the overall ANSI-136.

The current Cellular Data Packet Data (CDPD) networks offers a limited

data rate of about 19.2 kbps. In February 1999, the North American GSM Alliance and UWCC signed an interoperability agreement. They agreed a common core network for packet based data to bridge the difference between the existing IS 41 and GSM MAP core technologies. This agreement will allow today's TDMA and GSM networks to inter-operate as well as providing the basis for TDMA and GSM to follow the same migration path to 3G by first adopting IS136+ and then IS136HS/ EDGE COMPACT. IS136+ increases data rates to 64 kbps. This is achieved through software upgrades in the core CDPD network. IS136+ is very similar to GPRS for GSM, except that it is a circuit/packet hybrid rather than only packet. Also, the UWCC has introduced a spectrum efficient version of EDGE that will support the 384 kbps mandated packet data rates. But it will require only minimum spectral clearing and therefore could work for network operators with limited spectrum allocations.

### 1.3.3 CDMA Data Evolution

CDMA is evolving to 3G in the following steps:

CDMA path to 3G

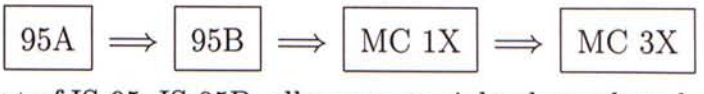


A refinement of IS-95, IS-95B, allows up to eight channels to be combined for packet-data rates as high as 64 kbps. Beyond IS-95B, CDMA evolves into 3G technology in a standard called cmda2000. cmda2000 comes in two phases. The first, with a specification already completed, is 1XRTT, while the next phase is 3XRTT. The 1X and 3X refer to the number of 1.25 MHz wide radio carrier

channels used, and RTT refers to radio-transmission technology. cdma2000 includes numerous improvements over IS-95A, including more sophisticated power control, new modulation on the reverse channels, and improved data encoding methods. The result is significantly higher capacity for the same amount of spectrum, and indoor data rates up to 2Mbps that meet the IMT-2000 requirements. The full-blown 3XRTT implementation of CDMA requires a 5MHz spectrum commitment for both forward and reverse links. However, 1XRTT can be used in existing CDMA channels since it uses the same 1.25 MHz bandwidth. 1XRTT can be deployed in existing spectrum to double voice capacity, and requires only a modest investment in infrastructure. It will provide IP-based packet-data rates of up to 144 kbps. Initial deployment of 1XRTT is expected by US CDMA carriers in 2001, with 3XRTT following a year or two behind, depending on whether new spectrum becomes available.

## 1.4 UTRA

The third-generation of mobile communications is approaching fast; the preliminary decision on the choice of access schemes for UMTS Terrestrial Radio Access (UTRA), was made by ETSI in January '98 and the ITU standardization process for IMT-2000 is now well underway. R&D departments world-wide are working around the clock on third-generation systems design, implementation, evaluation and trials. Licensing and regulatory preparations are proceeding in many countries, anticipating launch of service in 2002.

3rd Generation is the generic term used for the next generation of mobile communications systems. 3G systems will provide enhanced services to those -

such as voice, text and data - predominantly available today. UMTS is a part of the International Telecommunications Union's (ITU's) 'IMT-2000' vision of a global family of third-generation mobile communications systems. The technology concepts for 3rd Generation systems and services are currently under development industry wide. (3GPP)[1] is developing technical specifications for IMT-2000, the International Telecommunication Union's (ITU) framework for third-generation standards. 3GPP is a global co-operation between six Organizational Partners (ARIB, CWTS, ETSI, T1, TTA and TTC) who are recognized as being the world's major standardization bodies from Japan, China, Europe, USA and Korea. UTRA support both TDD and FDD operation with harmonised radio parameters between the modes.

### 1.4.1 UTRA FDD

UTRA FDD is a wideband direct sequence CDMA system, i.e. users are separated by different spreading codes and continuous transmission is used. The basic transmission unit in the resource space is the code. Multiple rates are achieved through variable spreading factors and multicode in both uplink and downlink. Bit rates from a few kbps up to 2Mbps can be provided with good bit rate granularity. FDD has a system chip rate of 3.84Mcps. This allows chip generation from a common clock, and this common clock can also be used as a GSM mobile station reference clock. The carrier spacing is 5MHz, with a carrier raster of 200KHz. The frequency bands for FDD downlink signal and uplink signal is either 2110 – 2170MHz and 1920 – 1980MHz, or 1930 – 1990MHz and 1850 – 1910MHz.

### Frame Structure

The frame structure in UTRA FDD is different in uplink and downlink. In the uplink, data (*dedicated physical data channel*, DPDCH) and control channels (*dedicated physical control channel*, DPCCH) are I/Q multiplexed as shown in figure 1.2, whereas in the downlink data and control channels (*dedicated physical channel*, DPCH) are time multiplexed as shown in figure 1.3. The super frame length is defined as 720ms= 6×120ms as an integer multiple of the corresponding GSM super frame for backward compatibility reasons. The slots corresponding to power uplink, only pilot symbols can be used if coherent detection is applied.

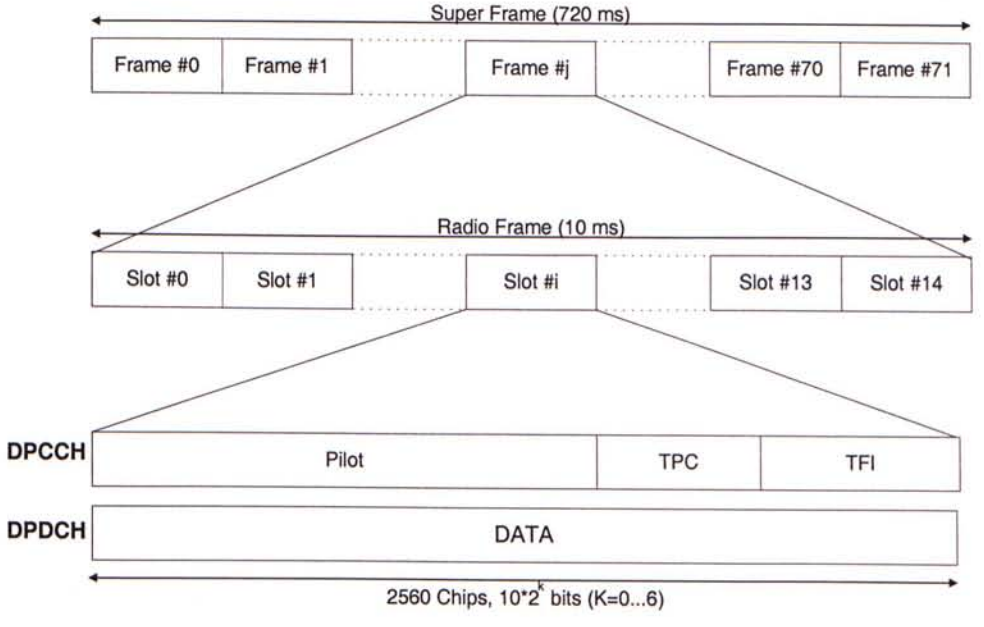


Figure 1.2: Frame structure for FDD uplink

In both, uplink and downlink spreading with a variable spreading factor in the range 4 to 256 (up to 512 in compressed mode) is applied depending on the data rate and service. In figure 1.4, the I/Q multiplexed DPDCH and DPCCH in the uplink are QPSK modulated. Each channel is scrambled with a

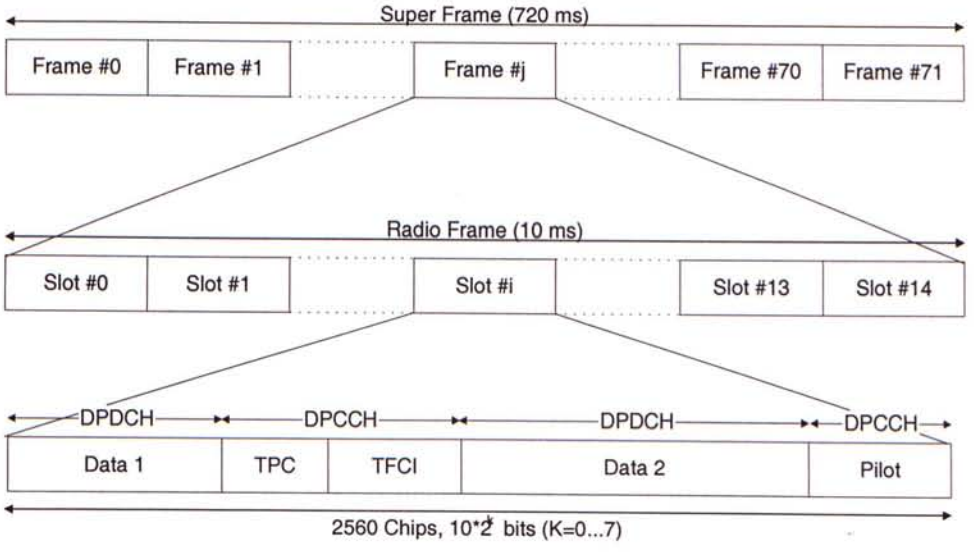


Figure 1.3: Frame structure for FDD downlink

specific code $C_d$ for DPDCH and $C_c$ for DPCCH and then scrambled with a UE specific code $C_{scramb}$ to distinguish different UEs. Each data channel DPDCH is assigned its own channleization code. The spreading/modulation for downlink is shown in figure 1.5. Each bit of DPCCH/DPDCH is first multiplied with a $2^k$ chips long channelization code ($C_C$ and $C_D$), where $k$ is related to the number of bits per frame of the physical channel (a $2^k$ chips long channelization code corresponds to $150 \times 2^{8-k}$ bits/frame). The channelization codes are assigned from the code tree in figure 1.6. This code tree is called the OVSF (*Orthogonal Variable Spreading Factor*) tree and it maintains orthogonal transmission on the downlink for different spreading factors of different DPCH.

Before scrambling, the spread physical channel is assigned to either the I branch or Q branch where it, after individual weighting, is added together with other physical channels. For the special case of a single PDCH plus one PCCH, the PDCH and PCCH should be assigned to the I and Q branch respectively.

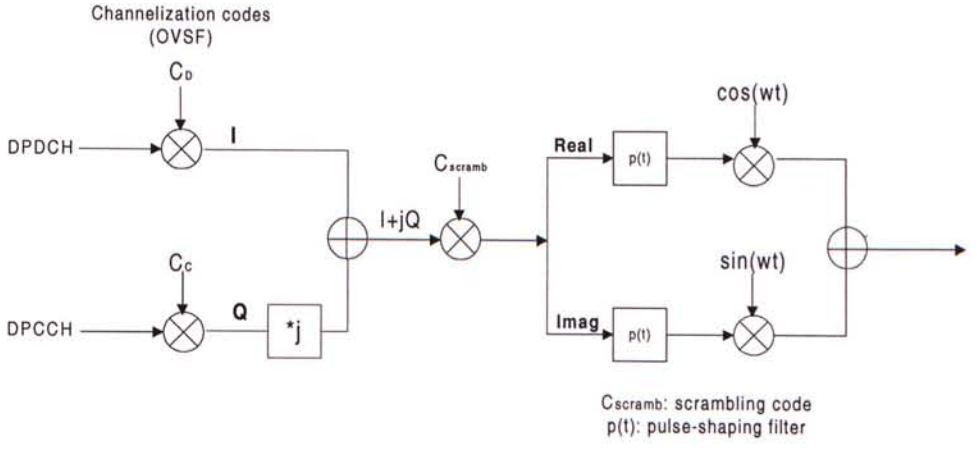


Figure 1.4: Spreading/modulation for FDD uplink

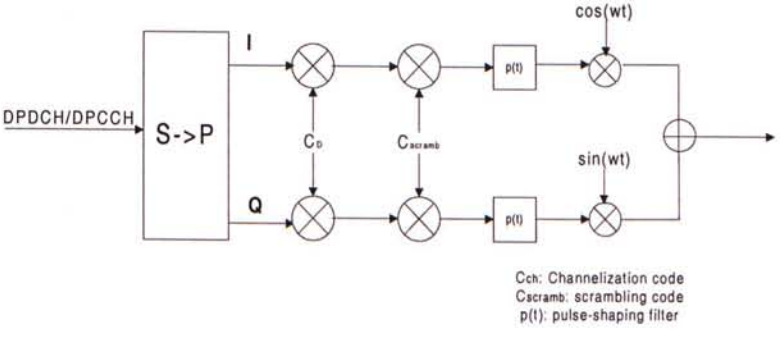


Figure 1.5: Spreading/modulation for FDD downlink

The allocation of codes from the code tree in figure 1.6 follows the following restrictions:

A PDCH that is to be transmitted on the I (Q) branch may use a certain code in the tree if and only if no other physical channels to be transmitted on the I (Q) branch are using a code that is on an underlying branch or on the path to the root of the tree. For a PCCH the restriction is that a certain code may be used if and only if no other physical channels to be transmitted on the I or Q branch are using code that is on an underlying branch or on the path to the root of the tree. The reason for stronger restrictions for the PCCH is

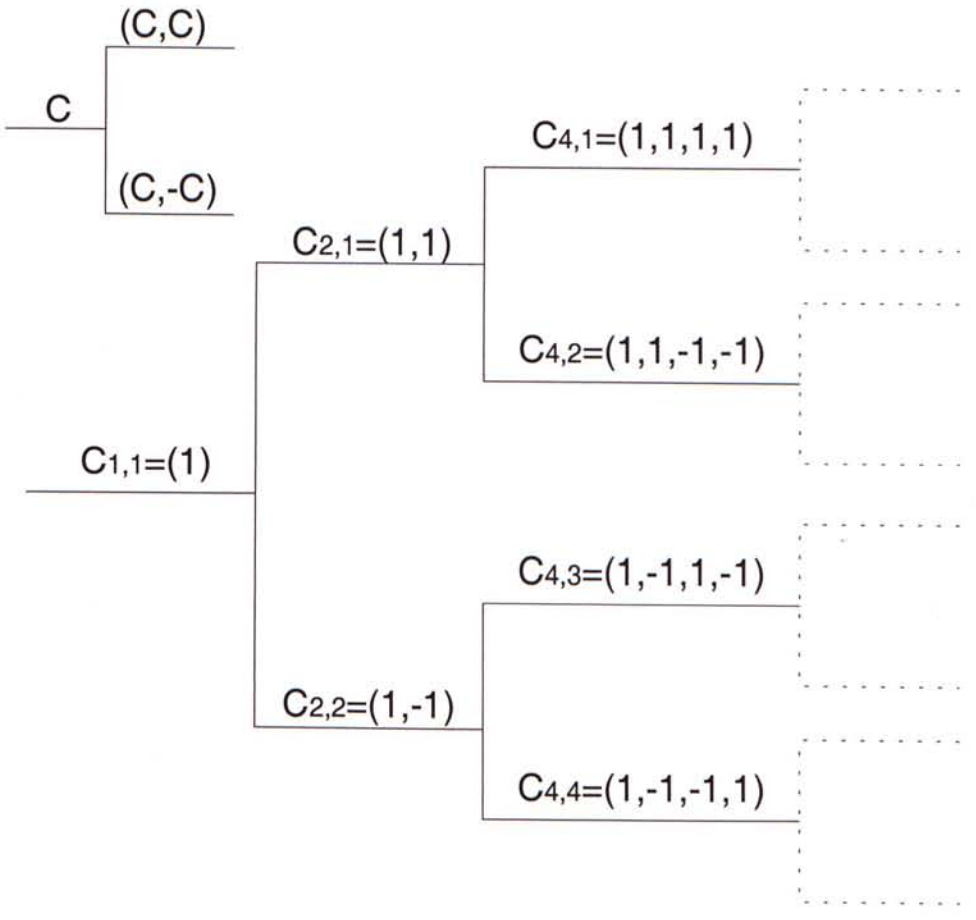


Figure 1.6: Channelization code tree. Top left shows the tree construction principle.

that physical channels transmitted with the same channelization codes on the I and Q branches respectively cannot be separated before the PCCH has been detected and channel estimates are available.

On the downlink, multiple codes are transmitted with possibly different spreading factors for the different channels DPCH depending on the service. The data modulation is QPSK. Spreading is performed by channelization codes $C_{ch}$ for each DPCH and a cell specific scrambling code $C_{scramb}$ to distinguish different cells. Each addition downlink DPCH in the case of multicode transmission

is modulated in the same way.

The pilot channel is simply an IQ pair, transmitting the downlink scrambling codes on both branches. Equivalently one may say that the pilot channel is two physical channels with all ones, spread to the chip rate with the all-ones channelization codes. Thus, all-one coes cannot be used for channelization of any other physical channel in the downlink, since there would be interference with the pilot channel.

### Random Access

In IMT-2000 WCDMA FDD system, random access transmissions are based on a Slotted ALOHA approach with fast acquisition. There are two types of random access channels in FDD system, they are *physical random access channel* (PRACH) and *physical common packet access channel* (PCPCH).

The random burst of PRACH and PCPCH consists a preamble part and a message part. When user wants to send data in random access channel, he should first send a preamble coded with a signature with collision risk in the *access slot* (AS) and waits for the positive, negative acknowledgment or time-out event. After the user gets a positive acknowledgment result from the *acquisition indicator channel* (AICH) , and then he can send the message part with contention free. There are a total of 16 signatures, and 15 access slots per 20ms frame in the system. The number of accessible signatures and access slots are indicated in a number of *access service classes* (ASC) broadcasted in the BCCH. Both PRACH and PCPCH can have different ASCs.

### The RACH structure

The structure of the Random-Access burst is shown in figure 1.7. The Random-Access burst consists of two parts, a preamble part of length of $16 \times 256$ chips (1ms) and a message part of 10ms length.

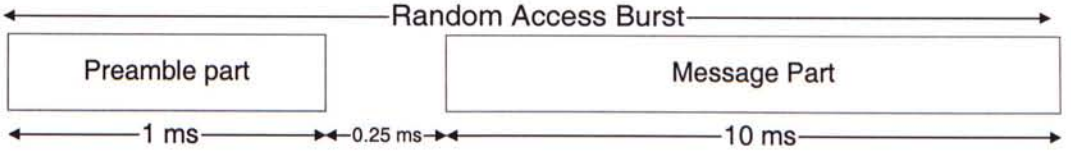


Figure 1.7: Structure of the Random Access Burst

The preamble part of the random-access burst consists of a *signature* of length 16 complex symbols (the *preamble sequence*), see figure 1.8. Each preamble symbol is spread by an Orthogonal Gold code (the *preamble code*) of length 256 chips. The preamble sequence is randomly chosen from a set of 16 orthogonal code words of length 16. All 16 different signatures are available in each cell and can be transmitted at the same time. Neighboring base stations use different preamble codes and information about what preamble code(s) are available in each cell is broadcast on the BCCH.

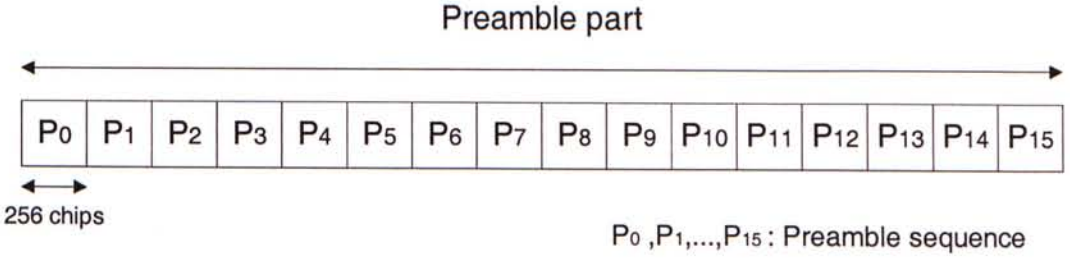


Figure 1.8: Structure of the Random Access Burst preamble

Figure 1.9 shows the structure of the message part of the Random-Access burst. The message part have two types, 10 ms and 20 ms in length. The 10 ms

message part is split into 15 slots, each of length 2560 chips. Each slot consists of two parts, a data part that carries Layer 2 information and a control part that carries Layer 1 control information. The data and control parts are transmitted in parallel. A 20 ms long message part consists of two consecutive message part radio frames.

The data part at each slot consists of $10 \times 2^k$ bits, where $k = 0, 1, 2, 3$. This corresponds to a spreading factor of $256, 128, 64$, and 32 respectively for the message data part. Therefore, the data rate will be $150, 300, 600$, and 1200 bits per 10 ms frame.

The control part consists of 8 known pilot bits to support channel estimation for coherent detection and 2 TFCI bits. This corresponds to a spreading factor of 256 for the message control part. The total number of TFCI bits in the random-access message is $15 \times 2 = 30$. The TFCI value corresponds to a certain transport format of the current Random-access message.

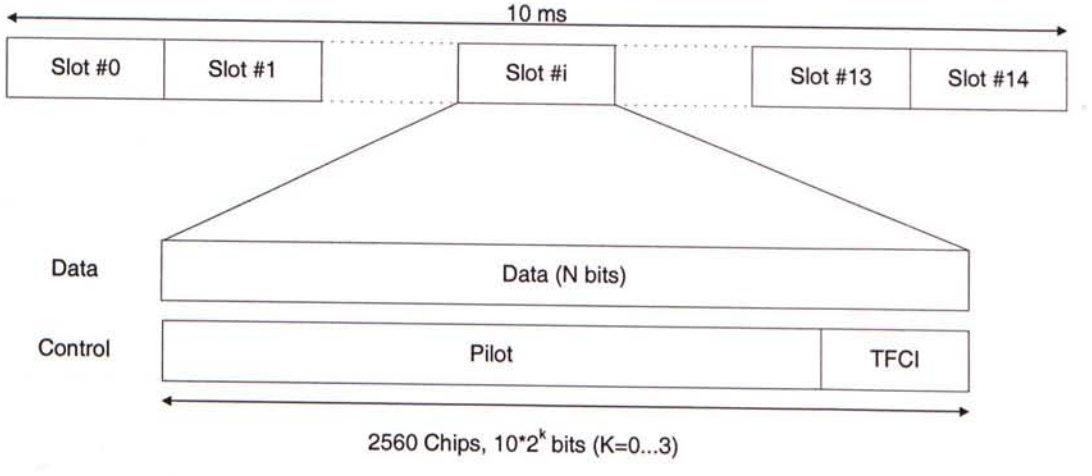


Figure 1.9: The RACH message part structure

Table 1.1 shows the data rate for the RACH message part with different spreading factor.

| Slot Format #i | Channel Bit Rate (kbps) | Channel Symbol Rate (kbps) | SF | N (Bits/Slot) |
|---|---|---|---|---|
| 0 | 15 | 15 | 256 | 10 |
| 1 | 30 | 30 | 128 | 20 |
| 2 | 60 | 60 | 64 | 40 |
| 3 | 120 | 120 | 32 | 80 |

Table 1.1: Random-access message fields

### Acquisition Indicator Channel (AICH)

The Acquisition Indicator channel (AICH) is a physical channel used to carry Acquisition Indicators (AI). Acquisition Indicator AIs corresponds to signatures on the PRACH or PCPCH. Note that for PCPCH, the AICH either corresponds to an access preamble or a CD preamble. The AICH corresponding to the access preamble is an AP-AICH and the AICH corresponding to the CD preamble is a CD-AICH. The AP-AICH and CD-AICH use different channelization codes.

Figure 1.10 illustrates the structure of the AICH. The AICH consists of a repeated sequence of 15 consecutive access slots (AS), each of length 40 bit intervals. Each access slot consists of two parts, an Acquisition-Indicator (AI) part consisting of 32 real-valued symbols $A_0$,..., $A_{31}$ and an unused part consisting of 8 real-valued symbols $A_{32}$,..., $A_{39}$. The phase reference for the AICH is the Primary CPICH.

### The RACH procedure

when a UE wants to send control message or the data message on the PRACH or PCPCH. It should

1. Get the available Access slots and the available signatures for sending the preamble. These information are broadcast on the BCCH. The available

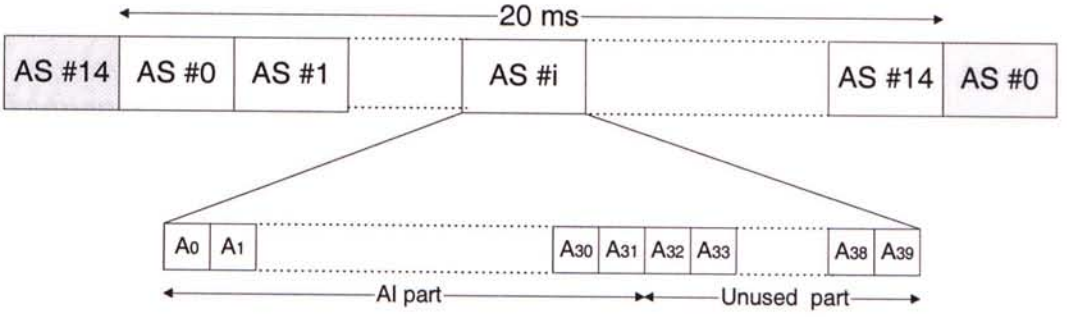


Figure 1.10: The Structure of the AICH

number of access slots are describe as the RACH sub-channel.

2. Send the preamble with a signature, in any of the access slots (depends of the class for the message part, e.g. preamble for control message. can be sent in every frame and the preamble for the data message can only be sent in the odd or even frame).

3. Set a timer and wait for either the negative ACK or positive ACK. If no ACK(both negative or positive) are received within a particular time period. It should increase the power and resend the preamble again. UE should quit this procedure after a few failed trails.

4. Wait for the positive or the negative ACK from the AICH carried in the FACH (it takes 2 or 3 access slot time/at least 0.25ms). The AICH only carry the successful signature numbers. If a negative ACK is received, then quit this procedure.

5. If a positive ACK is received, then the message part can be sent with a channelization code corresponding to one of the 16 sub-tree of the OVSF tree. So there are only 16 different message parts being sent within a 10 ms or 20 ms time period.

### 1.4.2 UTRA TDD

#### Frequency bands and channel arrangement

The frequency bands for the TDD downlink signal and uplink signal is either 1900 – 1920 MHz and 2010 – 2025 MHz, 1850 – 1910 MHz and 1930 – 1990 MHz, or 1910 – 1930 MHz. No TX-RX frequency separation is required as TDD is employed. Each TDMA frame consists of 15 time slots where each time slot can be allocated to either transmit(downlink) or receive(uplink). The channel spacing is 5Mhz and the channel raster is 200KHz.

#### Physical Channels

A physical channel is defined as the association of one code, one time slot and one frequency. All physical channels take three-layer structure with respect to time slots, radio frames and *system frame numbering* (SFN). Depending on the resource allocation, the configuration of radio frames or time slots becomes different. The physical channel signal format is presented in figure 1.11. All physical channels need guard symbols in every time slot. The time slots are used in the sense of a TDMA component to separate different user signals in the time and the code domain.

A physical channel in TDD is a burst, which is transmitted in a particular time slot within allocated Radio Frames. The allocation can be continuous, i.e. the time slot in every frame is allocated to the physical channel or discontinuous, i.e. the time slot in a subset of all frames is allocated only. A burst is the combination of a data part, a midamble and a guard period. The duration of a burst is one time slot. Several bursts can be transmitted at the same time

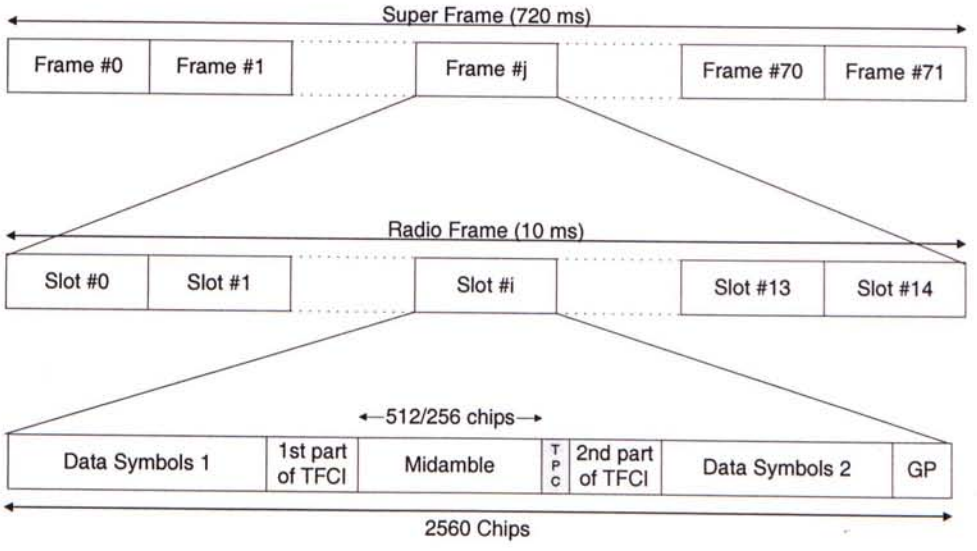


Figure 1.11: TDD physical channel signal format

from one transmitter. In this case, the data part must use different OVSF channelization codes, but the same scrambling code. The midamble part has to use the same basic midamble code, but can use different midambles.

The TDMA frame has a duration of 10 ms and is subdivided into 15 time slots. Each time slot corresponds to 2560 chips. Each 10 ms frame consists of 15 time slots, each allocated to either the uplink or the downlink, illustrated in figure 1.12. With such a flexibility, the TDD mode can be adapted to different environments and deployment scenarios. In any configuration at least one time slot has to be allocated for the downlink and at least one time slot has to be allocated for the uplink.

Some of the second generation systems, e.g. GSM, the boundary between the uplink and the downlink in a frame is not movable frame by frame. With this restriction, system cannot use the uplink-time slot for transferring the queued data in the BS buffer when the uplink traffic is very low. It results wasted

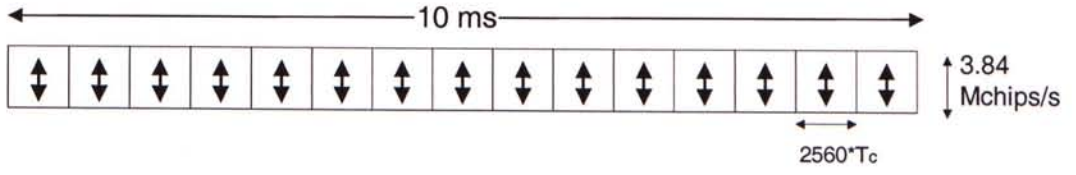


Figure 1.12: The TDD frame structure

bandwidth. By moving the boundary every frame, we can maximum the channel usage. It is very usefully when the highly asymmetric Internet traffic is applied to the system, the DL to UL traffic ratio can reach upto 13 : 1. Two examples for multiple and single switching point configurations for asymmetric UL/DL allocations are given in figure 1.13 and figure 1.14 .

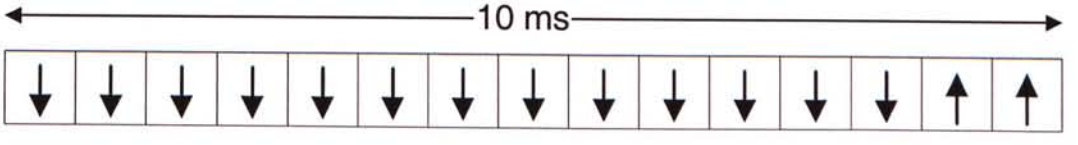


Figure 1.13: Single-switching-point configuration

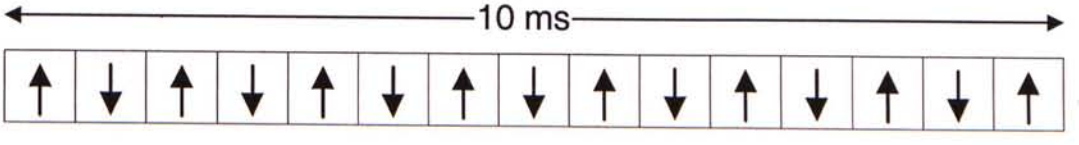


Figure 1.14: Multiple-switching-point configuration

Spreading is applied to the data part of the physical channels and consists of two operations. The first is the channelization operation, which transforms every data symbol into a number of chips, thus increasing the bandwidth of the signal. The number of chips per data symbol is called the *Spreading Factor* (SF). The second operation is the scrambling operation, where a scrambling code is applied to the spread signal.

Downlink physical channels shall use $SF = 16$. Multiple parallel physical

channels can be used to support higher data rates. These parallel physical channels shall be transmitted using different channelization codes. Operation with a single code with spreading factor 1 is possible for the downlink physical channels. Uplink physical channels can use spreading factor ranging from 16 down to 1. For multicode transmission a UE shall use a maximum of two physical channels with different channelization codes per time slot simultaneously.

Burst Type 1 and the Burst Type 2 are defined. Both consist of two data symbol fields, a midamble and a guard period. Bursts Type 1 has a longer midamble of 512 chips than Burst Type 2 with a midamble of 256 chips. Because of the longer midamble, Burst Type 1 is suited for the uplink, where up to 16 different channel impulse responses can be estimated. Burst Type 2 can be used for the downlink and, if the bursts within a time slot are allocated to less than four users, also for the uplink. The data fields of Burst Type 1 are 976 chips long, whereas the data fields length of Burst Type 2 are 1104 chips long. The corresponding number of symbols(bits) depends on the spreading factor, as indicated in table 1.2. The guard period for the Burst Type 1 and 2 is 96 chip periods long.

Table 1.2: Number of symbols per data field in Bursts Type 1 and 2.

| Spreading factor | Number of symbols per data field in Burst 1 | Number of symbols per data field in Burst 2 |
|---|---|---|
| 1 | 976 | 1104 |
| 2 | 488 | 552 |
| 4 | 244 | 276 |
| 8 | 122 | 138 |
| 16 | 61 | 69 |

### Primary Common Control Physical Channel (P-CCPCH)

The P-CCPCH uses fixed spreading with a spreading factor $SF = 16$. Burst Type 1 is used for the P-CCPCH. No TFCI is applied for the P-CCPCH. The position (time slot / code) of the P-CCPCH is known from the Physical Synchronization Channel (PSCH).

### Secondary Common Control Physical Channel (S-CCPCH)

The S-CCPCH uses fixed spreading with a spreading factor $SF = 16$. Burst Types 1 or 2 are used for the S-CCPCHs. TFCI may be applied for S-CCPCHs. PCH and FACH are mapped onto one or more secondary common control physical channels (S-CCPCH).

### Physical Random Access Channel (PRACH)

The UE send the uplink access bursts randomly in the PRACH. The uplink PRACH use either spreading factor $SF = 16$ or $SF = 8$. The set of admissible spreading codes for use on the PRACH and the associated spreading factors are broadcast on the BCH. The PRACH burst consists of two data symbol fields, a midamble and a guard period. The second data symbol field is shorter than the first symbol data field by 96 chips in order to provide additional guard time at the end of the PRACH time slot. The access burst is depicted in figure 1.15, the contents of the access burst fields are listed in table 1.3.

### Physical Synchronization Channel (PSCH)

In TDD mode code group of a cell can be derived from the synchronization channel. Additional information, received from higher layers on SCH transport

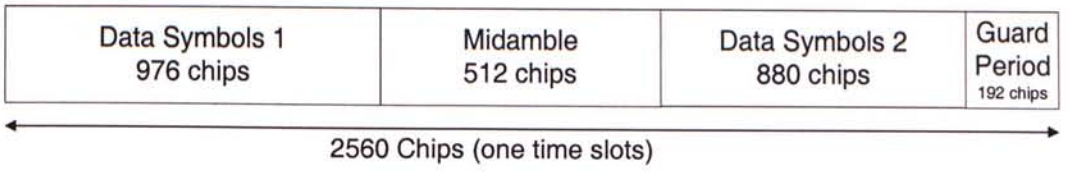


Figure 1.15: TDD Physical Random Access Channel burst

| Spreading Factor | Number of symbols in data field 1 | Number of symbols in data field 2 |
|---|---|---|
| 8 | 122 | 110 |
| 16 | 61 | 55 |

Table 1.3: The contents of the PRACH burst field

channel, is also transmitted to the UE in PSCH in case 3 from below. In order not to limit the uplink/downlink asymmetry the PSCH is mapped on one or two downlink slots per frame only.

There are three cases of PSCH and P-CCPCH allocation as follows:

Case 1) PSCH and P-CCPCH allocated in TS#$k$, $k = 0, ..., 14$.

Case 2) PSCH allocated in two TS: TS#$k$ and TS#$k + 8$, $k = 0, ..., 6$; P-CCPCH allocated in TS#$k$.

Case 3) PSCH allocated in two TS, TS#$k$ and TS#$k + 8$, $k = 0, ..., 6$, and the P-CCPCH allocated in TS#$i$, $i = 0, ..., 6$, pointed by PSCH. Pointing is determined via the SCH from the higher layers.

These three cases are addressed by higher layers using the SCCH in TDD Mode. The position of PSCH (value of $k$) in frame can change on a long term basis in any case. Due to this PSCH scheme, the position of PCCPCH is known from the PSCH.

### Physical Uplink Shared Channel (PUSCH)

For Physical Uplink Shared Channel (PUSCH) the burst structure of DPCH as described in section 1.4.2 shall be used. User specific physical layer parameters like power control, timing advance or directive antenna settings are derived from the associated channel (FACH or DCH). PUSCH provides the possibility for transmission of TFCI in uplink.

### Physical Downlink Shared Channel (PDSCH)

For Physical Downlink Shared Channel (PDSCH) the burst structure of DPCH as described in section 1.4.2 shall be used. User specific physical layer parameters like power control or directive antenna settings are derived from the associated channel (FACH or DCH). PDSCH provides the possibility for transmission of TFCI in downlink.

To indicate to the UE that there is data to decode on the DSCH, three signalling methods are available:

1) using the TFCI field of the associated channel or PDSCH.

2) using on the DSCH user specific midamble derived from the set of midambles used for that cell.

3) using higher layer signalling.

When the midamble based method is used, the UE shall decode the PDSCH if the PDSCH was transmitted with the midamble indicated for the UE by UTRAN.

### The Page Indicator Channel (PICH)

PICH is a physical channel used to carry the Page Indicators (PI). The PICH substitutes one or more paging sub-channels that are mapped on a S-CCPCH. The page indicator indicates a paging message for one or more UEs that are associated with it.

## 1.4.3 Transport Channels

Transport channels are the services offered by Layer 1 to the higher layers. A general classification of transport channels is into two groups: dedicated transport channels and common transport channels. Dedicated Channels (DCH) is the only type of dedicated transport channel. It is possible to use beamforming, change rate fast(each 10ms), and use enhanced power control and inherent addressing of UEs. The Common Transport Channels and their characters are list in figure 1.16. Figure 1.17 shows the mapping relationship between transport channels and physical channels.

| Random Access Channel (RACH) | Forward Access Channel (FACH) | Broadcast Control Channel (BCCH) | Paging Channel (PCH) | Synchronisation Channel (SCH) |
|---|---|---|---|---|
| • Existence in uplink only.<br>• Collision risk.<br>• Open loop power control.<br>• Limited data field.<br>• Requirement for in-band identification of the UEs. | • Existence in downlink only.<br>• Possibility to use beamforming.<br>• Possiblity to use enhanced power control.<br>• Reuqirement for in-band identification of UEs. | • Existence in downlink only.<br>• Low fixed bit rate.<br>• Requirement to be broadcast in the entire coverage area of the cell. | • Existence in downlink only.<br>• Possibility for sleep mode procedures.<br>• Requirement to be broadcast in the entire coverage area of the cell. | • Existence in TDD and downlink only<br>• Low fixed bit rate.<br>• Requirement to be broadcast in the entire coverage area of the cell. |

Figure 1.16: TDD Common transport channels

| **Transport Channels** | maps to | **Physical Channels** |
|---|---|---|
| DCH | ---------- | Dedicated Physical Channel (DPDCH) |
| BCH | ---------- | Primary Common Control Physical Channel (P-CCPCH) |
| FACH<br>PCH | ---------- | Secondary Common Control Physical Channel (S-CCPCH) |
| RACH | ---------- | Physical Random Access Channel (PRACH) |
| SCH | ---------- | Physical Synchronization Channel (PSCH) |
| USCH | ---------- | Synchronization Channel (SCH) |
| DSCH | ---------- | Physical Downlink Shared Channel (PDSCH)<br>Page Indicator Channel (PICH)<br>Synchronization Channel (SCH) |

Figure 1.17: Transport channel to physical mapping

# Chapter 2

# Spreading Factor Optimization for FDD Downlink

The OVSF codes are valuable resources in CDMA system. In FDD downlink, all downlink channels share a set of codes from an OVSF tree. There are a total of 512 physical channels with SF=512 in the FDD downlink, each can carry 10 bits per time slot (equivalent to a data rate of 150 kbps). For convenience, we call this 10 bits per time slot a *Bandwidth Unit* (BU). Thus, the total FDD downlink capacity is 512 BUs. The spreading factor of each physical channel should be at least 4 as required by the standard[4]. Each physical channel can have a spreading factor $2^i$, where $i = 4, 3, ..., 9$. Thus, each physical channel can carriy $2^i$ BUs, where $i = 0, 1, ..., 7$. For example, if 48 BUs are requested by a UE, the scheduler should assign two physical channels, one has a SF=32 and the other one has a SF=16, for this UE to avoid bandwidth wastage.

An arbitrary payload of size $b$ can be represented as a $k$-bit binary number $\mathbf{b} = (b_{k-1}b_{k-2}\cdots b_1 b_0)$, where $k = \lceil \log_2(b+1) \rceil$. In other words, $b = \sum_{i=0}^{k-1} b_i \cdot 2^i$.

Also, let $u(\mathbf{b})$ be the number of physical channels needed for payload b without bandwidth wastage. It is clear that $u(\mathbf{b})$ is simply the number of 1's in $\mathbf{b}$.

The standard specifies that each UE can use up to 6 physical channels on the downlink. The maximum number of physical channel $m$ that a particular UE can use is obviously dependent on the MIPS power of the UE receiver. For convenience, we call $m$ the channel splitting factor of a UE. For example, if a UE with $m = 2$ requests a logical channel of 9 BUs, the scheduler can assign two physical channels, one with 8 BUs and one with 1 BUs, for this UE. However, if the UE can only use one physical channel ($m = 1$ ) , one 16 BU physical channel needs to be used. This results in a wastage of $\frac{16-9}{16} = 43.75\%$.

## 2.1 The Optimal Channel Splitting Problem

In this section, we propose an algorithm for finding the optimal channel splitting for a given $b$ and $m$. Optimal here means minimum bandwidth wastage. Given payload size $b$ , we want to find the bandwidth size $b'$ with minimum bandwidth wastage. We denote the binary formats of $b$ and $b'$ as $\mathbf{b}$ and $\mathbf{b}'$, respectively. If $m \geq u(\mathbf{b})$, there exists sufficient physical channels for $\mathbf{b}$. Hence, we set $\mathbf{b}'$ = $\mathbf{b}$. On the other hand, if $m < u(\mathbf{b})$, a code set with slightly larger weight is required to accommodate $u(\mathbf{b})$. In the other word, the payload portion of the lowest order bits in $\mathbf{b}$ will need to be aggregated to one of the higher bit in $\mathbf{b}'$. In doing so, some bandwidth wastage on downlink will result. The algorithm for finding the optimal channel splitting is given in figure 2.1 .

As an example, let $\mathbf{b}$ = 1011010 and $m = 3$. We can see that $u(\mathbf{b}) = 4$ , which is larger than $m$. First, we add a binary number 1000 to $\mathbf{b}$, and we have

| | |
|---|---|
| Inputs: | Payload $b = (b_{k-1}b_k \cdots b_0)$ and maximum number of splits $m$. |
| Outputs: | Bandwidth $b' = (b'_{k-1}b'_k \cdots b'_0)$ |
| Step 1: | If $(u(b) \leq m)$ set $b' = b$, then goto END |
| Step 2: | [When $u(b) > m$ ] |
| Step 2.1: | Set $i$ be the bit position of the $m$th 1, $i = 0, 1, ..., k-1$. |
| Step 2.2: | $b' = b$. |
| Step 2.3: | $b' = b' + 1\overbrace{00...000}^{\text{i bits}}$. |
| Step 2.4: | $b' = b' \oplus 11...1\overbrace{0...0}^{\text{i bits}}$, where $\oplus$ is logical AND operation. |
| END: | $b'$ is obtained. [END] |

Figure 2.1: The Optimal Channel Splitting Algorithm

$\mathbf{b'} = 1101010$. Then do a binary **AND** operation with 1111000. In other words, we set the last 3 bits to '0'. At last, we have $\mathbf{b'} = 1100000$ and it has two 1, i.e., $u(b') < m$. These steps are listed below:

$$\begin{array}{rl} 1011010 & \mathbf{b} \\ \underline{+0001000} & \\ 1100010 & \\ \underline{\oplus 1111000} & \\ 1100000 & \mathbf{b\prime} \end{array}$$

From $\mathbf{b'}$, we can see that two physical channels, one with $2^6$-BU and one with $2^5$-BU, are assigned for $\mathbf{b}$.

Now, we see how does $m$ affect the average wastage. We assume the sizes of the requested downlink decicated channels are uniformly distributed between 1 and 128. Figure 2.2 shows the average wastage for the channel assignments of different $m$'s. The average wastage drops from 24.9% with $m = 1$ to 9.8% with $m = 2$. Moreover, the average wastage is almost zero when $m = 4$. Thus, with larger $m$, the channel wastage can be decreased and the channel efficiency can also be increased.

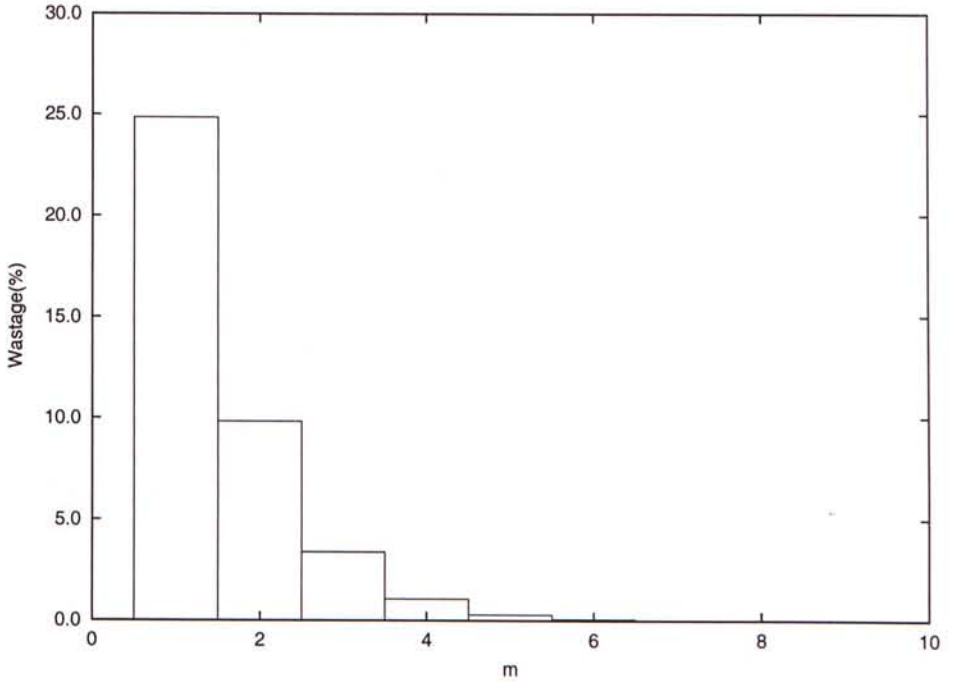


Figure 2.2: The average wastage with $m$ as a pramaeter while the payloads are uniformly distributed between 1 and 128.

## 2.2 Spreading Factor Optimization for FDD Downlink Dedicated Channel

Circuit switch traffic, such as voice call, video conferencing, and fax, will be the major traffic in 3G system. We know that the average wastage is 24.9% if each UE can only receive one DCH in each time slot. As a result, the downlink capacity utilization will be very poor. If the traffic load is light, we can afford this wastage. But when the traffic load is high, we have no choice but to drop some DCH requests, although 24.9% downlink capacity is unused. From the result of pervious section, we know that the average wastage decreases as $m$ increases. Therefore, we should assign as much DCHs as possible (up to $m$) to

| | |
|---|---|
| Inputs: | Payload $b$ (the size of the requested logical channel), $m = 1$ |
| Outputs: | Two DCHs, $CH_1$ and $CH_2$, of two successive frames. |
| Step 1: | Find the size of the DCHs with miniminzed wastage, . $s_1$ and $s_2$, for $b$ with $m = 2$. |
| Step 2: | $CH_1$ is a $2 * s_1$-BU DCH, $CH_2$ is a $2 * s_2$-BU DCH. [END] |

Figure 2.3: Channel assignment algorithm with changable spreading factor.

| | Frame i | Frame i+1 | Frame i+2 | Frame i+3 | Frame i+4 |
|---|---|---|---|---|---|
| m=1 | 128-BU | 128-BU | 128-BU | 128-BU | ··· |
| m=2 | 64-BU+ 32-BU | 64-BU+ 32-BU | 64-BU+ 32-BU | 64-BU+ 32-BU | ··· |

Figure 2.4: Channel assignments for the request of 92-BU logical channel with $m = 1$ and $m = 2$.

each request. But if all UEs have only $m = 1$, the average wastage is still 24.9%. In this section, we propose a simple algorithm to reduce the average wastage by changing the spreading factor of DCHs frame by frame.

Considering all UEs have $m = 1$, a large average wastage will only occur when the spreading factor of all the DCHs are unchanged during the whole transmission periods. In our algorithm, we change the spreading factor frame by frame. By doing so, the average wastage can be decreased. The algorithm is shown in figure 2.3 and we illustrate it by the following example.

Let a user with $m = 1$ requests for a 92-BU channel. Since we can only assign him a 128-BU channel, the wastage is $\frac{128-92}{128} = 28.1\%$ . But if this user can use two DCHs(i.e., $m = 2$) at the same time, the average wastage drops to $\frac{(64+32)-92}{64+32} = 4.2\%$. The assignment are shown in figure 2.4.

In figure 2.5, we interchange the 32-BU channel of Frame $i$ with the 64-BU

| | Frame i | Frame i+1 | Frame i+2 | Frame i+3 | Frame i+4 |
|---|---|---|---|---|---|
| m=2 | 64-BU+ 32-BU↗ | ↙64-BU+ 32-BU | 64-BU+ 32-BU↗ | ↙64-BU+ 32-BU | ··· |
| m=2 | 64-BU+ 64-BU | 32-BU+ 32-BU | 64-BU+ 64-BU | 32-BU+ 32-BU | ··· |
| m=1 | 128-BU | 64-BU | 128-BU | 64-BU | ··· |

Figure 2.5: Inter-changing with the DCHs of two successive frames.

channel of Frame $i+1$. So, we have two 64-BU channels in Frame $i$ and two 64-BU channels in Frame $i+1$. Since two 64-BU channels can be grouped into one 128-BU channel and two 32-BU channels can also be grouped into one 64-BU channel. We have one 128-BU channel and one 64-BU channel in Frame $i$ and $i+1$, respectively. By doing so, the average wastage for the assignment in Frame $i$ and $i+1$ is only $\frac{(128+64)-92*2}{(128+64)} = 4.2\%$, same as that of $m = 2$ in the fixed spreading factor assignment. We do the same changes in the other frames. As a result, the average wastage is much smaller than 28.1% in the fixed spreading factor assignment. For decreasing the complexity of our algorithm, we only inter-change the DCHs of two successive frames. Moreover, we only perform the interchanging procedure when $m$ is 1. Although this algorithm is simple, it can reduce the average wastage from 24.9% to 9%. Compared with the fixed spreading factor assigment, the overhead is almost none.

We should try to assign $u$ ($b$) DCHs for each request. But when a UE can only use one DCH(i.e. $m = 1$), we can use the inter-changing method. As a result, the maximum wastage will be less than 10% (i.e., same as $m = 2$ in fixed spreading factor assignment).

# Chapter 3

# Random Access Channel Stability Control

## 3.1 Random Access Slotted Aloha

### 3.1.1 System model

In UTRA TDD system, each time slot in a frame can either be used for uplink or downlink. We call the set of time slots assigned to uplink as the uplink part and those assigned for the downlink as the downlink part. The uplink part is shared by random bursts and data bursts. As a Base Station can correctly receive only up to 8 bursts in each uplink time slot, the collision of data/random bursts is inevitable if the total number exceeds 8. We call this a time-collision. To reduce the probability of collision, data bursts and random bursts should be separated as far as possible into different time slots, giving rise to the data part and random access part. In this chapter, we focus only on the random access

transmissions. A UE with a random access burst to transmit will first choose a channelisation code randomly from the available code set $C = \{c_1, c_2, ..., c_M\}$ broadcast on BCH. If multiple UEs choose the same code in the same time slot, a code-collision occurs. However, this collision has no effect on the other UEs choosing codes in the same time slot.

### 3.1.2 Probability of Code-Collision

Let $x$ be the number of random access transmissions at particular random access slot and let $A = \{c_i | c_i \in C\}$ be the set of codes chosen for contention. We call $A$ the *contention code-set*. Table 3.1 shows some typical $A$'s and their respective collision-free codes. Suppose the $x$ transmissions are from $UE_1$,$UE_2$,...,and

| $A$ | Collision-Free codes |
|---|---|
| $\{c_{35}, c_{12}, c_{49}, c_{35}\}$ | $c_{12}, c_{49}$ |
| $\{c_{21}, c_{21}, c_{26}, c_{13}, c_{13}\}$ | $c_{26}$ |
| $\{c_{17}, c_{17}, c_{32}, c_{32}, c_{32}, c_{17}\}$ | none, due to code-collision |
| $\{c_{12}, c_{21}, c_{20}, c_{21}, c_{12}, c_{12}, c_{20}, c_{20}\}$ | none, due to code-collision |
| $\{c_{32}, c_{21}, c_{13}, c_2, c_{17}, c_{19}, c_4, c_{30}, c_{23}\}$ | none, due to time-collision |

Table 3.1: Sets of $A$ and their respective collision-free codes.

$UE_X$. Let $c_i$ be the chosen code by $UE_j$. Then the condition for collision-free is that the other $(x-1)$ UEs do not select $c_i$. In other words, their code choices is limited to $M-1$. With this restriction, the total number of choices they have is $(M-1)^{x-1}$. Figure 3.1 shows all choices of $UE_2$,...,and $UE_x$. Since the choices of $c_i$(there are $M$ of them) and $UE_j$(there are $x$ of them) are arbitrary, the total number of collision-free codes in all arrangements of the $x$ codes in $A$ is

$$N_{cf} = M \cdot x \cdot (M-1)^{x-1}.$$

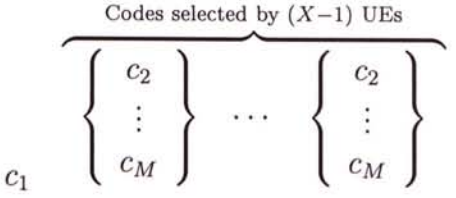


Figure 3.1: $UE_1$ select code $c_1$.

Since each of the $x$ codes in a contention code-set $A$ is chosen randomly from the $M$ codes in $C$, the total number of different contention codes arrangements is $M^x$. As each code arrangement consists of $x$ codes, the total number of codes in all arrangements of the $x$ codes in $A$ is

$$N_t = x \cdot M^x.$$

It is now easy to see that the collision-free probability $P_{cf}(x)$ is simply

$$P_{cf}(x) = \frac{N_{cf}}{N_t} = (1 - \frac{1}{M})^{x-1}, \text{ for } x \leq 8. \tag{3.1}$$

Then, the collision probability is $P_c(x) = 1 - P_{cf}(x)$. Table 3.2 shows an example with $x = 4$ and $M = 3$. The total number of codes in all arrangements is 324 and the total number of collision-free codes is 96. Thus, the probability of collision-free is $P_{cf}(x = 4)|_{M=3} = \frac{96}{324} = 0.296$. Figure 3.2 shows the probability of collision-free versus number of simultaneously transmitted random access bursts $X$ with number of available codes $M$ as a parameter. We can see that the probability of collision-free is higher than 0.8 and 0.9 when $M = 32$ and $M = 128$ for $X \leq 8$, respectively. If we have the maximum available codes $M_{\max} \geq 128$, we set $M = 128$. Otherwise, $M = 32$ is not a bad choice.

Table 3.2: All possible arrangements of $A$ for $x = 4$ and $M = 3$. The collision-free codes are marked by "$\square$".

| | | |
|---|---|---|
| $\{c_1, c_1, c_1, c_1\}$ | $\{c_1, c_1, c_1, \boxed{c_2}\}$ | $\{c_1, c_1, c_1, \boxed{c_3}\}$ |
| $\{c_1, c_1, \boxed{c_2}, c_1\}$ | $\{c_1, c_1, c_2, c_2\}$ | $\{c_1, c_1, \boxed{c_2}, \boxed{c_3}\}$ |
| $\{c_1, c_1, \boxed{c_3}, c_1\}$ | $\{c_1, c_1, \boxed{c_3}, \boxed{c_2}\}$ | $\{c_1, c_1, c_3, c_3\}$ |
| $\{c_1, \boxed{c_2}, c_1, c_1\}$ | $\{c_1, c_2, c_1, c_2\}$ | $\{c_1, \boxed{c_2}, c_1, \boxed{c_3}\}$ |
| $\{c_1, c_2, c_2, c_1\}$ | $\{\boxed{c_1}, c_2, c_2, c_2\}$ | $\{\boxed{c_1}, c_2, c_2, \boxed{c_3}\}$ |
| $\{c_1, \boxed{c_2}, \boxed{c_3}, c_1\}$ | $\{\boxed{c_1}, c_2, \boxed{c_3}, c_2\}$ | $\{\boxed{c_1}, \boxed{c_2}, c_3, c_3\}$ |
| $\{c_1, \boxed{c_3}, c_1, c_1\}$ | $\{c_1, \boxed{c_3}, c_1, \boxed{c_2}\}$ | $\{c_1, c_3, c_1, c_3\}$ |
| $\{c_1, \boxed{c_3}, \boxed{c_2}, c_1\}$ | $\{\boxed{c_1}, \boxed{c_3}, c_2, c_2\}$ | $\{\boxed{c_1}, c_3, \boxed{c_2}, c_3\}$ |
| $\{c_1, c_3, c_3, c_1\}$ | $\{\boxed{c_1}, c_3, c_3, \boxed{c_2}\}$ | $\{\boxed{c_1}, c_3, c_3, c_3\}$ |
| $\{\boxed{c_2}, c_1, c_1, c_1\}$ | $\{c_2, c_1, c_1, c_2\}$ | $\{\boxed{c_2}, c_1, c_1, \boxed{c_3}\}$ |
| $\{c_2, c_1, c_2, c_1\}$ | $\{c_2, \boxed{c_1}, c_2, c_2\}$ | $\{c_2, \boxed{c_1}, c_2, \boxed{c_3}\}$ |
| $\{\boxed{c_2}, c_1, \boxed{c_3}, c_1\}$ | $\{c_2, \boxed{c_1}, \boxed{c_3}, c_2\}$ | $\{\boxed{c_2}, \boxed{c_1}, c_3, c_3\}$ |
| $\{c_2, c_2, c_1, c_1\}$ | $\{c_2, c_2, \boxed{c_1}, c_2\}$ | $\{c_2, c_2, \boxed{c_1}, \boxed{c_3}\}$ |
| $\{c_2, c_2, c_2, \boxed{c_1}\}$ | $\{c_2, c_2, c_2, c_2\}$ | $\{c_2, c_2, c_2, \boxed{c_3}\}$ |
| $\{c_2, c_2, \boxed{c_3}, \boxed{c_1}\}$ | $\{c_2, c_2, \boxed{c_3}, c_2\}$ | $\{c_2, c_2, c_3, c_3\}$ |
| $\{\boxed{c_2}, \boxed{c_3}, c_1, c_1\}$ | $\{c_2, \boxed{c_3}, \boxed{c_1}, c_2\}$ | $\{\boxed{c_2}, c_3, \boxed{c_1}, c_3\}$ |
| $\{c_2, \boxed{c_3}, c_2, \boxed{c_1}\}$ | $\{c_2, \boxed{c_3}, c_2, c_2\}$ | $\{c_2, c_3, c_2, c_3\}$ |
| $\{\boxed{c_2}, c_3, c_3, \boxed{c_1}\}$ | $\{c_2, c_3, c_3, c_2\}$ | $\{\boxed{c_2}, c_3, c_3, c_3\}$ |
| $\{\boxed{c_3}, c_1, c_1, c_1\}$ | $\{\boxed{c_3}, c_1, c_1, \boxed{c_2}\}$ | $\{c_3, c_1, c_1, c_3\}$ |
| $\{\boxed{c_3}, c_1, \boxed{c_2}, c_1\}$ | $\{\boxed{c_3}, \boxed{c_1}, c_2, c_2\}$ | $\{c_3, \boxed{c_1}, \boxed{c_2}, c_3\}$ |
| $\{c_3, c_1, c_3, c_1\}$ | $\{c_3, \boxed{c_1}, c_3, \boxed{c_2}\}$ | $\{c_3, \boxed{c_1}, c_3, c_3\}$ |
| $\{\boxed{c_3}, \boxed{c_2}, c_1, c_1\}$ | $\{\boxed{c_3}, c_2, \boxed{c_1}, c_2\}$ | $\{c_3, \boxed{c_2}, \boxed{c_1}, c_3\}$ |
| $\{\boxed{c_3}, c_2, c_2, \boxed{c_1}\}$ | $\{\boxed{c_3}, c_2, c_2, c_2\}$ | $\{c_3, c_2, c_2, c_3\}$ |
| $\{c_3, \boxed{c_2}, c_3, \boxed{c_1}\}$ | $\{c_3, c_2, c_3, c_2\}$ | $\{c_3, \boxed{c_2}, c_3, c_3\}$ |
| $\{c_3, c_3, c_1, c_1\}$ | $\{c_3, c_3, \boxed{c_1}, \boxed{c_2}\}$ | $\{c_3, c_3, \boxed{c_1}, c_3\}$ |
| $\{c_3, c_3, \boxed{c_2}, \boxed{c_1}\}$ | $\{c_3, c_3, c_2, c_2\}$ | $\{c_3, c_3, \boxed{c_2}, c_3\}$ |
| $\{c_3, c_3, c_3, \boxed{c_1}\}$ | $\{c_3, c_3, c_3, \boxed{c_2}\}$ | $\{c_3, c_3, c_3, c_3\}$ |

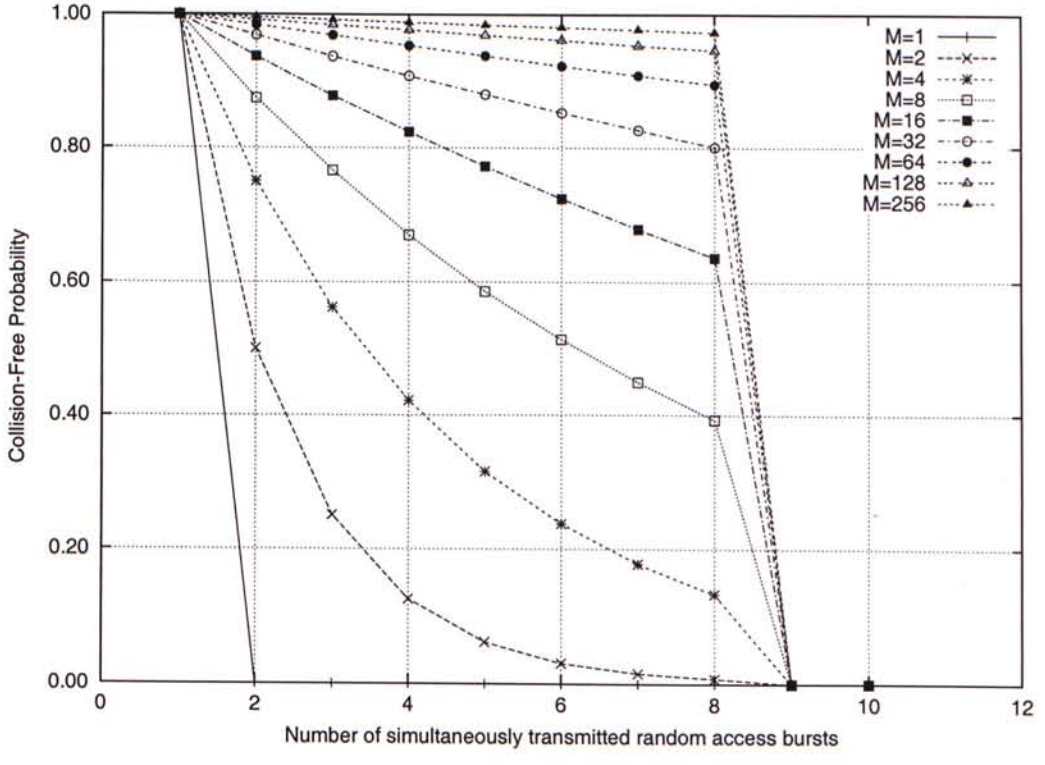


Figure 3.2: Collision-free Probability with $M$ as a parameter

### 3.1.3 Throughput Analysis of Random Access in TD/CDMA System

The random access protocol of UTRA TDD under study is modeled as a slotted ALOHA type system. In figure 3.3, let the arrivals of the new random access bursts be a Poisson process with rate $\lambda_N$. Let $\lambda_R$ be the rate of these collided bursts. Under the condition that the delay is sufficiently "random", it is a general practice to assume the combined new and retransmitted bursts is also a Poisson process with rate $\lambda = \lambda_N + \lambda_R$. As usual, we shall verify this by computer simulation. We assume thermal noise is negligible, and all unsuccessful transmissions are caused only by code collisions. Following the deviation in [5],

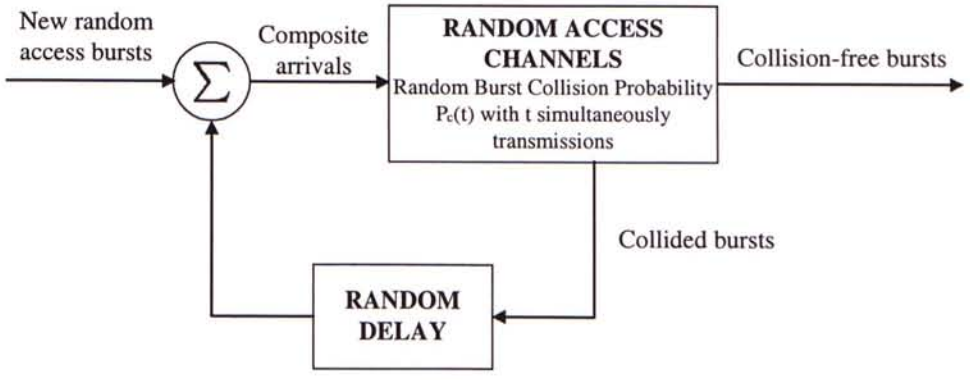


Figure 3.3: Random Access bursts flow diagram

let the number of attempted transmissions (composite arrivals) in the $j$th access slot be $T_j$. The probability that $S$ collision-free bursts of $t$ random access bursts in a particular random access slot is

$$Prob\{S = s|T = t\} = \binom{t}{s} P_{cf}{}^{t}(t) P_c{}^{t-s}(t)$$

We assume that the total number of arrivals is large enough to get a Poisson distribution function for the offered load. Therefore, the probability $f_T(t)$ that $t$ bursts are received by the Base Station during a certain random access slot is given by

$$f_T(t) = \frac{G^t}{t!} e^{-G}. \tag{3.2}$$

Here, $G$ is the average number of transmitted bursts per random access slot. We have $G = \lambda T_{slot}$, where $T_{slot}$ is the length of an random access slot in time. The steady-state throughput $S$ is the expected number of successful transmissions

per access slot. Thus,

$$\begin{aligned} S &= E[S] \\ &= E\left[E\left[S|T\right]\right] \qquad (3.3) \\ &= E\left[\sum_{s=0}^{T} s\binom{T}{s} {P_{cf}}^{s}(T){P_c}^{t-s}(T)\right] \\ &= E\left[\sum_{s=0}^{T} s\frac{T!}{(T-s)!s!}{P_{cf}}^{s}(T){P_c}^{t-s}(T)\right] \\ &= E\left[TP_{cf}(T)\sum_{s=0}^{T}\frac{(T-1)!}{(T-s)!(s-1)!}{P_{cf}}^{s-1}(T){P_c}^{t-s}(T)\right] \\ &= E\left[TP_{cf}(T)\cdot\left[P_{cf}(T)+P_c(T)\right]^{T-1}\right] \\ &= E\left[TP_{cf}(T)\right] \\ &= \sum_{t=1}^{\infty} tP_{cf}(t)f_T(t) \qquad (3.4) \end{aligned}$$

Substitute eq (3.2) into eq (3.4), we have

$$\begin{aligned} S &= \sum_{t=1}^{\infty} tP_{cf}(t)e^{-G}\frac{G^t}{t!} \\ &= Ge^{-G}\sum_{t=0}^{\infty}\frac{G^t}{t!}P_{cf}(t+1) \qquad \text{(bursts/slot)} \qquad (3.5) \end{aligned}$$

In figure 3.4, we can see that the throughput increases as $M$ increases. But it increases slowly after $M > 128$. Thus, $M = 128$ is a good choice for the system. We aslo get the throughput and effective delay for different $M$'s by computer simulation. The simulation model is identical to the analytical model. Results are shown in figure 3.4 and figure 3.5, respectively. We can see that simulation result of througput is almost as same as that of the analytical result.

Let the system throughput peaks at an offered load $G^*$. We can find $G^*$ for different $M$'s from both the analytical and simulation results. Since the offered

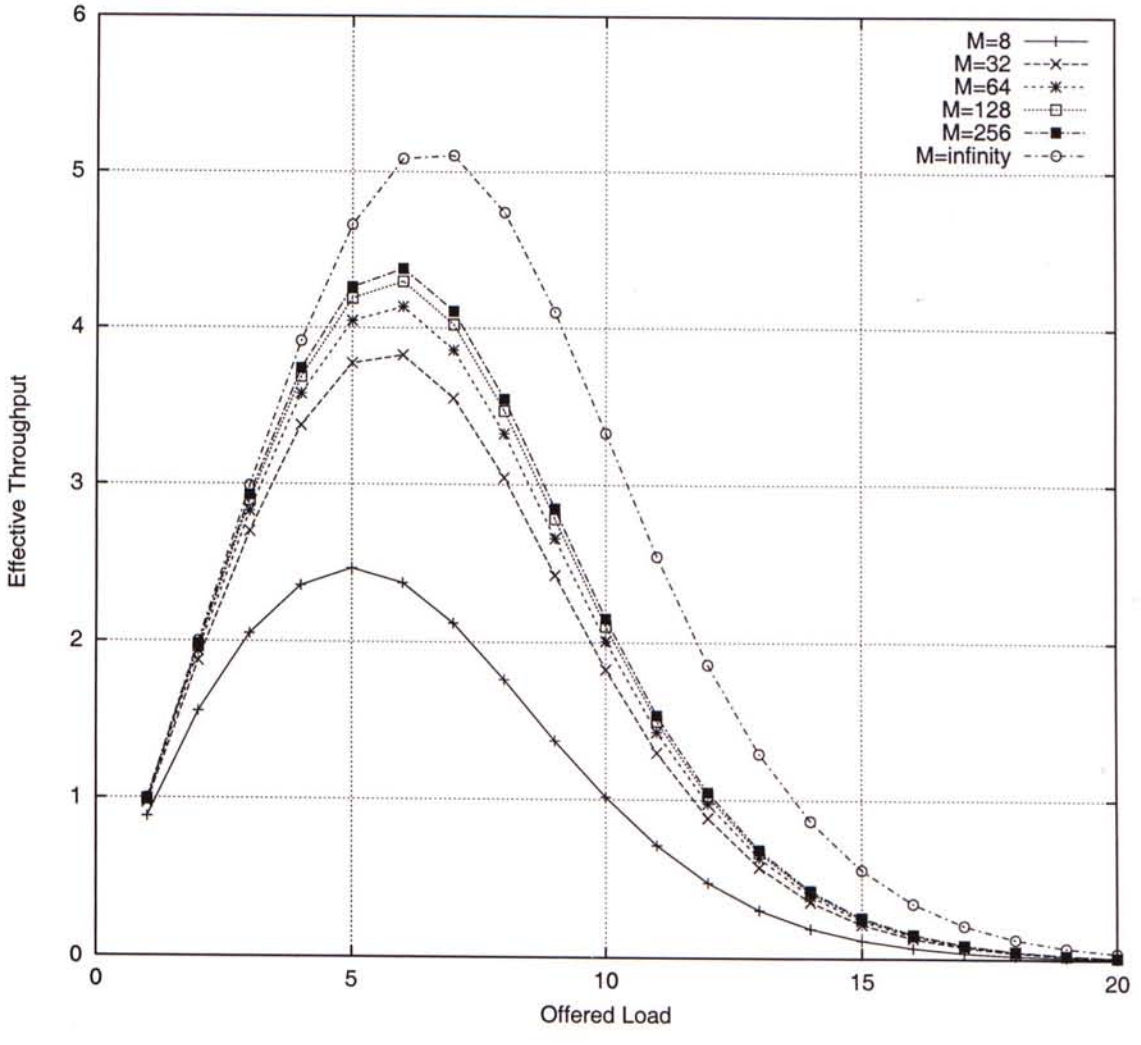


Figure 3.4: A comparison of the effective throughput versus offered load for different $M$'s.

load of the analytical result must be discreted because the term $P_{cf}(t+1)$ of eq (3.5) is a discrect function. We cannot get a precise value for $G^*$ from the analytical result hence we find $G^*$ from the simulation result. Table 3.3 lists different $G^*$ for different $M$'s.

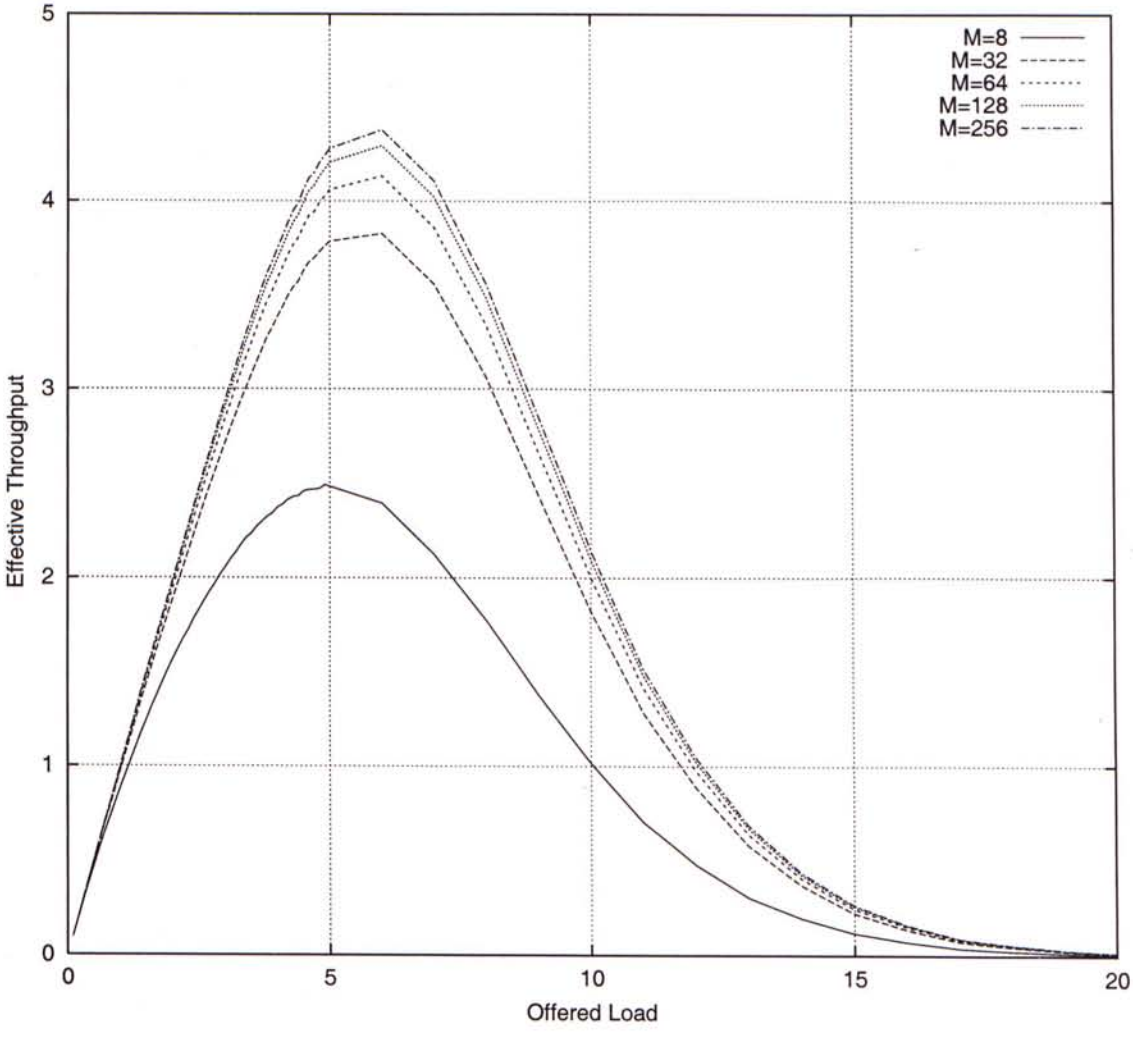


Figure 3.5: A comparison of the effective throughput versus offered load for different $M$'s.[Simulation Result]

Table 3.3: System throughput peaks at $G^*$ with $M$ as a parameter.

| Number of code ($M$) | 4 | 8 | 32 | 64 | 128 | 256 |
|---|---|---|---|---|---|---|
| Offered Load that achieves maximum throughput($G^*$) | 3.7 | 4.9 | 5.8 | 5.9 | 5.9 | 5.9 |

### 3.1.4 Retransmission

When UE's random access transmission is not successfully (i.e. collided with other bursts), it can retransmit this bursts with a random backoff delay. Here, we apply the 802.11 backoff delay procedure [2]. At each retransmission, the backoff time (in number of random access slots) is uniformly chosen in the range $(0, w-1)$. At the first retransmission, $w = W$(initial contenetion window). After each unsuccessful transmission, $w$ is double. UE retransmits the burst until it is received successfully.

### 3.1.5 System Delay

In our model, all collided bursts should be retransmitted. If the new random bursts arrival rate is too large, system will be unstable and the random access bursts delay will tend to infinity. Let $\delta$ be the maximum new random access bursts arrival rate before the system becomes unstable. We find $\delta$ with $M$ and $W$ as parameters by computer simulation. Here, we choose $M = 128$. Table 3.4 lists the approximate $\delta$ for different $W$. We also find the average delay for the random access bursts with $W$ as a parameter by computer simulation, result is shown in figure 3.6. From these results, we conclude that increasing $W$ do increase $\delta$ but also increase the average dealy. We choose $W = 256$ as the size of the initial contention window for our system in the following computer simulations of this chapter.

Table 3.4: Different $\delta$ with $W$ as a parameter when $M = 128$.

| $W$ | $\delta$ |
|---|---|
| 32 | 4.0 |
| 64 | 4.2 |
| 128 | 4.25 |
| 256 | 4.25 |
| 512 | 4.3 |
| 1024 | 4.4 |

## 3.2 Random Access Channel Stability Control

The UTRA TDD random access channel is a contention-based slotted ALOHA channel. As we can see in figure 3.4, the throughput decreases as the offered load increases. If we can maintain the combined rate of new and retransmitted bursts to be lower than $G^*$, system will be stable.

### 3.2.1 System Model

The stability control model is shown in figure 3.7. Hence, the arrival rate $\gamma$ of random access bursts is adjusted via access probability $P_a$. Different service classes can have different blocking probabilities. These probabilities control the permissions of accessing the PRACHs.

Figure 3.8 illustrates a possible frame structure for TDD random access. We assume that two time slots ($TS\#4$ and $TS\#11$) of each frame are used for the random access burst transmissions. Moreover, the BCCHs of two downlink slots are used for broadcasting the information needed for random access. For example, the BCCH of $TS\#2$ carries the number of available codes, the access

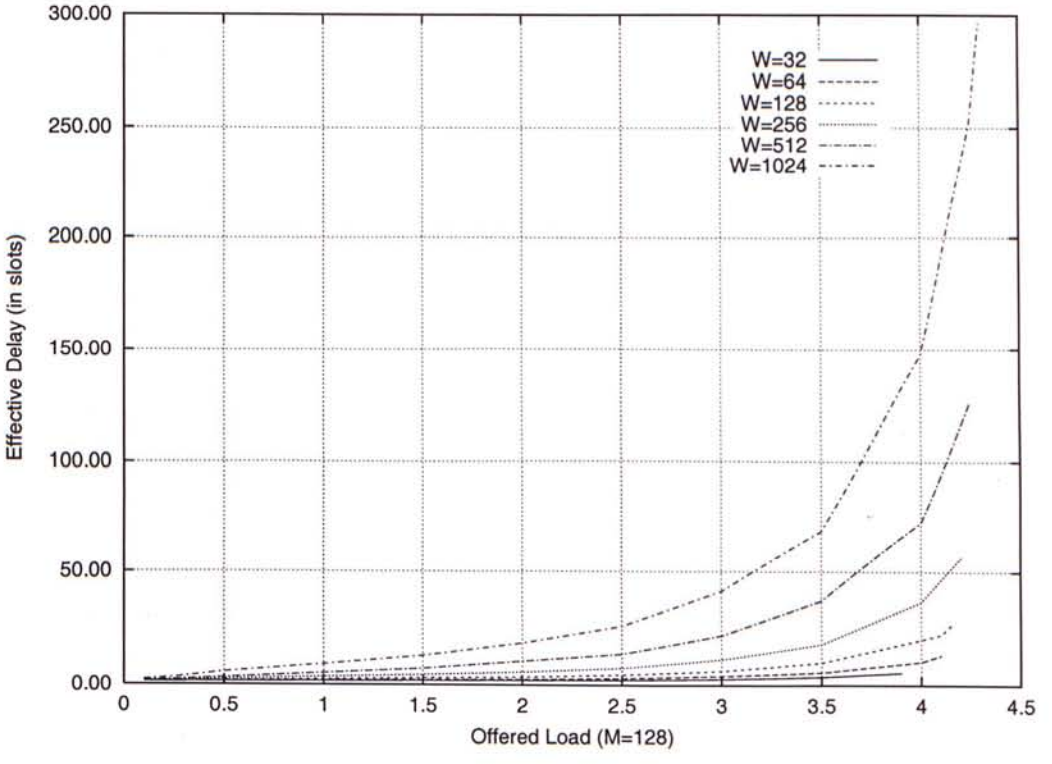


Figure 3.6: Thoughput-delay performance for different $W$.

probability for random access bursts , and the power control parameters. Moreover, some BCCHs of $TS\#2$ also carry the results of the transmissions in $TS\#11$ of the pervious frame. Also, the BCCHs in $TS\#9$ do the same functions. New arrival bursts and retransmitted bursts should use different midambles. Thus, they can be classfied by Base Station for the Stability Control.

### 3.2.2 Random Access Procedure

When a UE is in Idle mode, it will keep the downlink synchronisation and read the cell broadcast information. The random access information includes the channelization codes, spreading factor, midambles and the position of random access time slots. In our model, when a UE wants to transmit a burst on

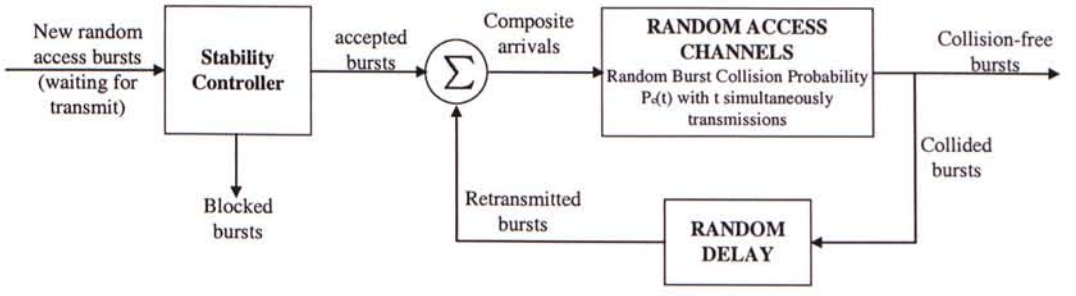


Figure 3.7: Random Access channel stability control model.

PRACH, it should first draw a number $R$ between 0 and 1. If $R$ is smaller than the access probability value corresponding to the service class of this burst, the UE gets the transmission permission. It then waits for the next random access slot and transmits the random access burst with a randomly chosen channelization code from the $M$ available codes. Otherwise, UE should drop this burst. The random access procedure is shown in figure 3.9.

Open-loop power control is used to adjust the transmit power of the physical random access burst transmission. Before the transmission of a random access burst, UE should measure the received power of the downlink Primary CCPCH over a sufficiently long time to remove effects of the non-reciprocal multi-path fading. From the power estimate and knowledge of the Primary CCPCH transmit power (broadcast on the BCCH) the downlink path-loss including shadow

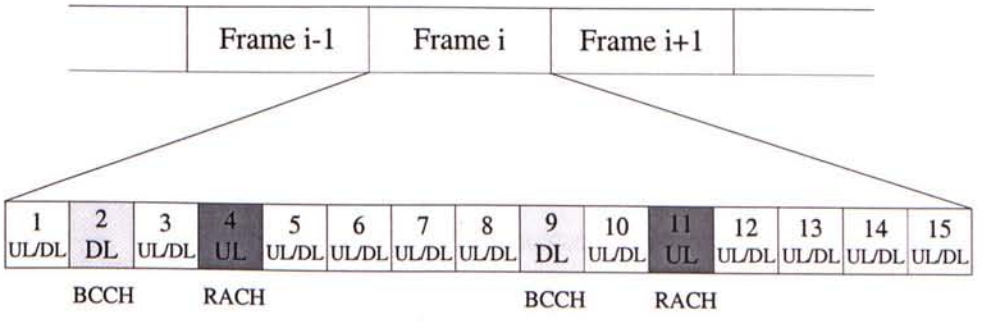


Figure 3.8: The frame structure

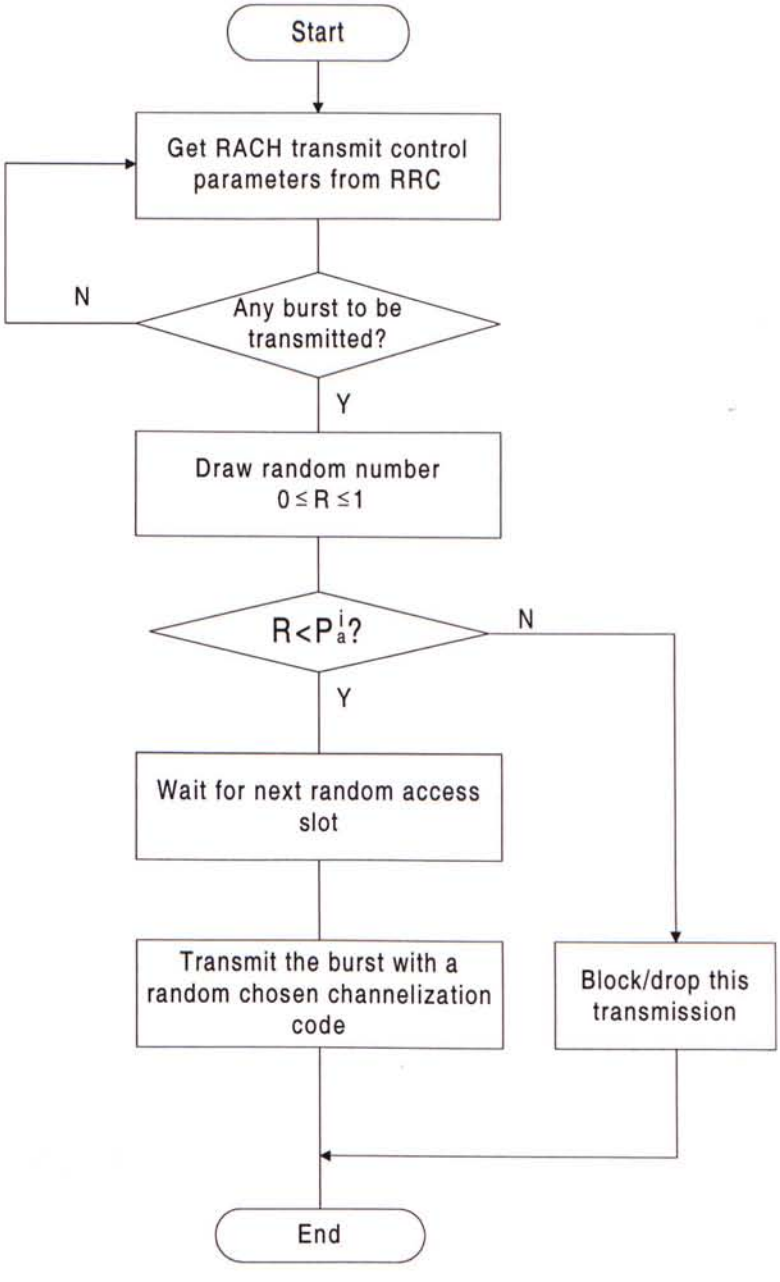


Figure 3.9: Random access procedure

fading can be found. From this path loss estimate and knowledge of the uplink interference level and the required received SIR, the transmitted power of the physical random access burst can be determined. The uplink interference level as well as the required received SIR are broadcast on the BCCH.

The result of the random access burst transmissions in a random access slot is broadcast on a BCCH one or few time slots later. If a burst is received by Base Station successfully (i.e., without code-collision), a number corresponding to the code used by this burst will be broadcast with a positive ACK. If Base Station receives a burst with poor BER, a number will be broadcast with a negative ACK. Otherwise, the burst may be collided with one or more bursts. In this situation, Base Station cannot know the codes used by these collided-bursts. Under the assumption of perfect power control (the received power from each UE is same at the Base Station), Base Station can estimate the number of received bursts by the total received power from the midamble parts of these bursts. Deducting the collision-free bursts, the number of collided bursts can be known. When UE get a negative ACK or no ACK for its random access bursts transmission. It can retransmit this bursts after a random backoff delay.

## 3.3 Random Access Channel Stability Control Alogrithm

We consider the UTRA TDD Slotted ALOHA system with infinite number of independent UEs sharing $M$ channelization codes for their random access burst transmissions. We know that the system throughput peaks at an offered load $G^*$ in figure 3.4. The new random access bursts arrive as a Poisson process of

rate $\gamma$, which may be a function of time. The retransmission rate of collided bursts is denoted as $R$. Let $G = \gamma + R$ be the composite arrival rate of new and retransmitted bursts. System is stable and has a maximum throughput if and only if $G \leq G^*$. If $\gamma$ is larger than the maximum system capacity $G^* - R$, the system will be unstable. If this happens, the algorithm should reduce the rate of new random access bursts by reducing the access probability $P_a$. By doing so, we have $G = P_a\gamma + R \leq G^*$ in the next random access slot and system is stable with a maximum throughput.

New arrival bursts and retransmitted bursts are the two types of bursts in the system. Retransmitted bursts are one of the major traffic of the system. If they can be received successfully as soon as possible, no further retransmissions are needed. By doing so, the average number of contention bursts in the following slots decreases and this can increases the capacity for new arrival bursts and decreases the code-collision probability. Otherwise, the retransmitted bursts and new arrival bursts will suffer from long delays. Also, we should not block the retransmission bursts hence their delays can be decreased. Therefore, the stability control algorithm should first reserve capacity for retransmitted bursts. However, the arrival rate of retransmitted bursts in next random access slot is unknown and we can only predict it from the measurement of the previous $u$ slots. The measurement may not be accurate when $u$ is small. On the other hand, when $u$ is too larger, the control may be too slow. Hence we need to find a suitable $u$ for our model later. Let $\widehat{R}(u)$ be the retransmitted bursts rate in the $u$ previous random access slots. We assume the retransmitted bursts arrival rate R in next random access slot is as same as $\widehat{R}(u)$. So, we set $R = \min\left(G^*, \widehat{R}(u)\right)$. The maximum arrival rate for the new arrival bursts $G$ is simply $G^* - R$.

Now, we go to find the blocking probability. Also, the number of new arrival bursts in next random access slot is unknown. We can find it with the help of the blocking probability. If Base Station received $m_i$ new burst in random access slots $i$, then, to a first approximation, there are about $n_i = \frac{m_i}{P_a}$ UEs requesting to access the RACH in this slot. Let $\widehat{A}(u)$ be the average number of new arrival bursts per slot over the previous $u$ random access slots. We have

$$\begin{aligned}\widehat{A}(u) &= \frac{\textit{Number of UEs want to access the RACH in previous u access slots}}{u} \\ &= \frac{\sum_{j=i-u+1}^{i} n_i}{u} \\ &= \frac{\sum m_i}{P_a \cdot u}\end{aligned}$$

Now, from the definition of $P_a$, it is clear that $P_a$ should be set such that

$$\widehat{A}(u)\, P_a = G^* - R$$

, or

$$\begin{aligned}P_a &= \frac{G^* - R}{\widehat{A}(u)} \\ &= \frac{G^* - \min\left(G^*, \widehat{R}(u)\right)}{\widehat{A}(u)}.\end{aligned}$$

The Random Access Channel Stability Control Algorithm is shown in figure 3.10.

### 3.3.1 Simulation

It is intractable to analysis the system with mathematical methods. Therefore, to obtain the performance of the stability control alogrithm, computer simulation studies have to be made.

| | |
|---|---|
| Step 1. | $G = G^* - \widehat{R}(u)$ |
| Step 2. | IF $G \leq 0$ THEN set $P_a = 0$ goto Step 4 |
| Step 3. | IF $\widehat{A}(u) \leq G$ THEN set $P_a = 1$ |
| | ELSE $P_a = \frac{G}{\widehat{A}(u)}$ |
| Step 4. | Broadcast the access probability $P_a$ |
| | [END] |

Figure 3.10: The Random Access Channel Stability Control Algorithm

We assume that no more than 8 bursts can be received correctly in each uplink time slot. There are $M$ available channelization codes can be used by the random access transmissions. In each frame, two slots are reserved for the random access.

### Traffic Model

We assume the bursts arrival is a Poisson process of constant rate $\gamma$. We also use the *sinusoidal arrival model* for our traffic model. In this model, the arrival rate of random access bursts is assumed to follow a sinusoidal curve during the simulation time, as shown in figure 3.11. The initial phase of the sinusoidal curve is distributed uniformly between 0 and $T$. The period is assumed to be $T$ minutes. Therefore, we have $\gamma(t) = \gamma \cdot \sin(t)$, $t \in [0, T]$. With perfect stability control, the rate of new arrival bursts should always be equal to or smaller than $G^*$. Thus, the arival rate of new bursts $f(t)$ is $\min[\gamma(t), G^*]$. Now, we go to find the average rate $h(f(t))$ of new arrival (non-blocked) bursts between $T$ minutes. We consider two different cases to derive $h(f(t))$.

Case A ($|G^* - \gamma| > 1$): Clearly, $h(f(t))$ is the either $\gamma$ or $G^*$. We have

$$h(f(t)) = \begin{cases} \gamma & , G^* - \gamma > 1 \\ G^* & , \gamma - G^* > 1 \end{cases}$$

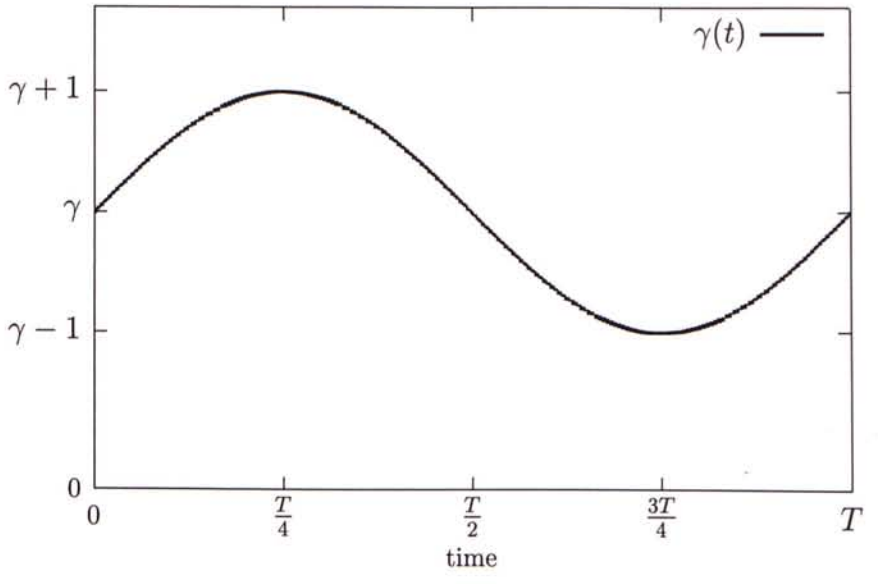


Figure 3.11: A sinusoidal arrival model for random access bursts

Case B ($|G^* - \gamma| \leq 1$): As shown in figure 3.12 and 3.13, $\gamma(t)$ and $y = G^*$ have cross points. Thus, $h(f(t))$ is the average height of the area under the bold curve of $f(t)$. Therfore we have,

$$h(f(t)) = \begin{cases} \frac{2\pi\gamma - 2\int_{\sin^{-1}(G^*-\gamma)}^{\frac{\pi}{2}}[(\sin t+\gamma)-G^*]dt}{2\pi} & , G^* \geq \gamma \\ \frac{2\pi G^* - 2\int_{\sin^{-1}(\gamma-G^*)+\pi}^{\frac{3\pi}{2}}[G^*-(\sin t+\gamma)]dt}{2\pi} & , G^* \leq \gamma \end{cases}$$

$$= \begin{cases} \frac{\pi\gamma-(\gamma-G^*)\left[\sin^{-1}(G^*-\gamma)-\frac{\pi}{2}\right]-\sqrt{1-(G^*-\gamma)^2}}{\pi} & , G^* \geq \gamma \\ \frac{\pi G^*-(\gamma-G^*)\left[\sin^{-1}(\gamma-G^*)-\frac{\pi}{2}\right]+\sqrt{1-(G^*-\gamma)^2}}{\pi} & , G^* \leq \gamma \end{cases}$$

In this section, only one class of random access bursts is considered. First, we generate the new random access bursts as a Poisson process of constant rate $\gamma$ (i.e., $\gamma(t) = \gamma$). Figure 3.14 shows the effective throughput for different $M$'s. The offered load is the arrival rate of the non-blocked new generated random access bursts. We can see that the offered load is limited by the maximum

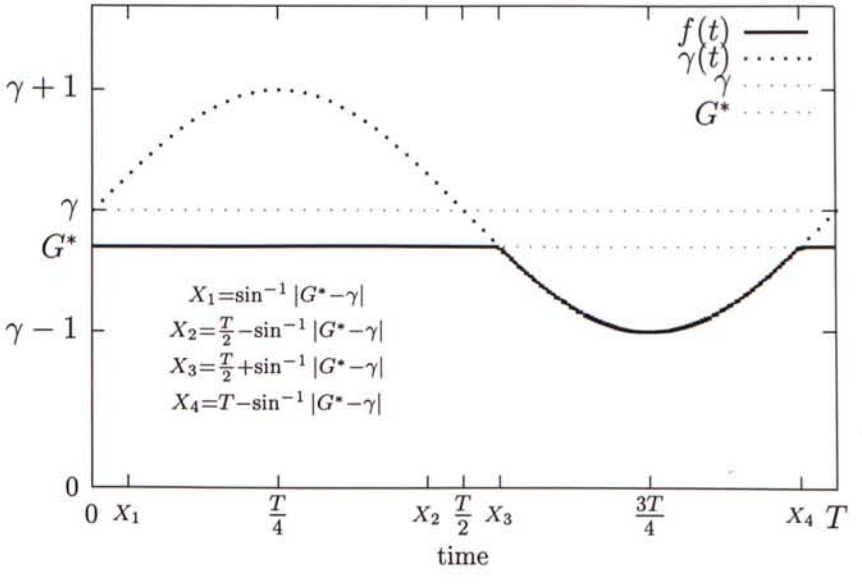


Figure 3.12: $f(t)$ is shown with $G^* - \gamma > 1$.

offered load $G^*$. Hence, the system is always stable and the throughput is near the maximum throughput. So, our Stability Control Algorithm is effective for offered load with constant arrival rate. In this figure, we can see that the maximum throughput increases with $M$. Figure 3.15 shows the mean random access delay as a function of offered load with different $M$'s. We can also see that the mean delay is a constant when offered load is larger than $G^*$. As the number of available codes $M$ increases, the maximum throughput increases but so does the average delay increases. From the simulation results, we observe that $M = 128$ is a suitable choice in terms of effective delay and the maximum throughput. Thus, for the following simulation experiments, we choose $M = 128$ throughout.

Next, we use the sinusoidal arrival model. We show the effective throughputs

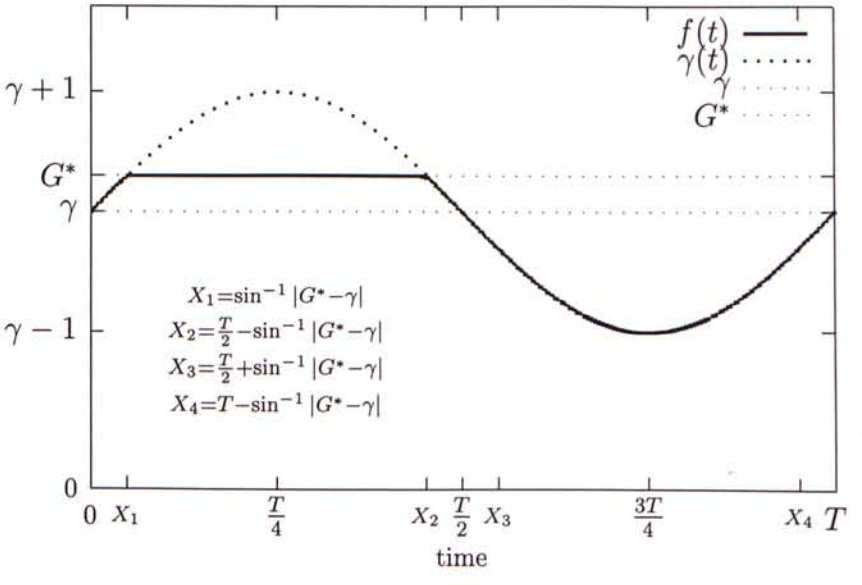


Figure 3.13: $f(t)$ is shown with $G^* - \gamma < 1$.

and check the stability of the system with some critical values of $\gamma$ for the function $\gamma(t) = \gamma \sin(t)$. They are $\gamma = 6.7, 6.2, 5.7, 5.2, 4.7, 4.2, 4, 3, 2$,and 1. When $\gamma = 6.7$, the curve of $\gamma(t)$ is larger than $y = G^*$ and there is no crossing point, we expect the effective throughput to be as same as the maximum throughput $G^*$. When $\gamma = 5.7$(i.e., $G^*$), the mean height of $\gamma(t)$ is as same as $G^*$. The curve of $\gamma(t)$ and $y = G^*$ has two crossing points when $\gamma = 6.2$ and 5.2. We expect the throughput for $\gamma = 5.7, 6.2$ and 5.2 to be same as that of $h(f(t))$. At last, we test with $\gamma = 4.7, 4.2, 4, 3, 2$, and 1, the expected effective throughputs are the same as that of $\gamma = 4.7, 4.2, 4, 3, 2$, and 1. In the simulation, we use $u = 100$ and we will discuss later how $u$ affects the effective throughtput and the system stability. Table 3.5 lists the results for the sinusoidal arrival model with different duration of the sinusoidal curve with $T = 1$, 5, and 15 minutes, while

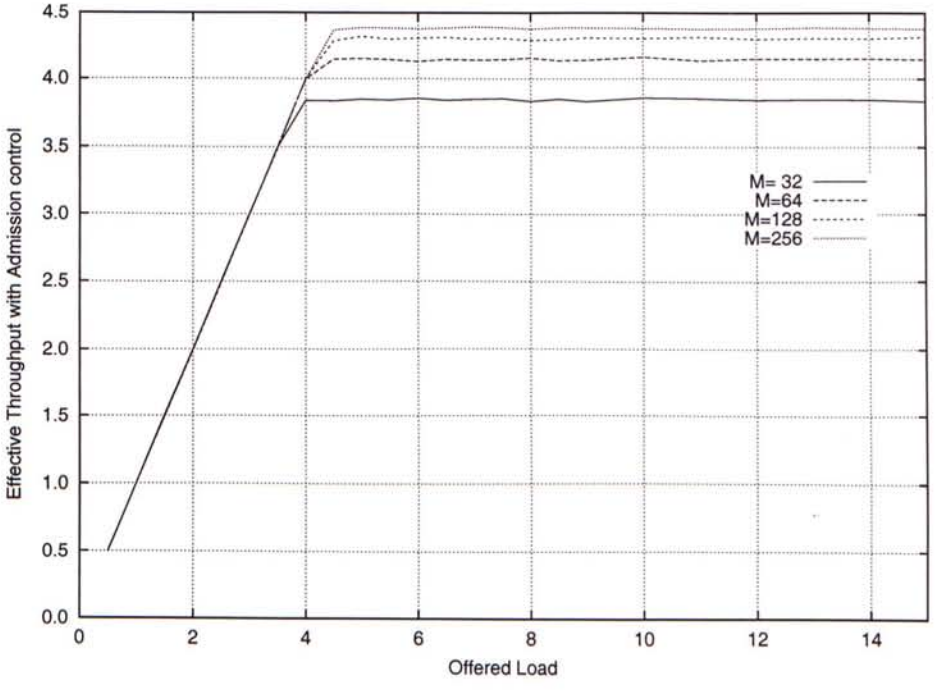


Figure 3.14: Effective throughput with stability control for different M.

the expected effective throughput can be obtained in figure 3.14 with $h(f(t))$ as the offered load. From the above results with two different traffic models, we conclude that our stablility control algorithm is robust enough to maintain the system in a stable state with maximum throughput. Now, we go back and see how $u$ affects the throughput and stability. We choose $T = 1$ minute and $\gamma = 6.7, 6.2, 5.7, 5.2, 4.7$, and 4 for the simulation. In table 3.6, when $u = 1$ (slot), we can see that the system throughputs are not good and the system is unstable for some $\gamma$ 's. So, we should not choose a small value for $u$. When $u = 1000$, the throughput drops because the number of blocked bursts increases while $\gamma(t)$ is rising although the system can accept these bursts. Also, we check the throughput for $\gamma(t) = \gamma$ with $u = 1$ as a parameter. But $u$ affects neither the throughput nor the system stability. Thus, we choose $u = 100$ (equivalent

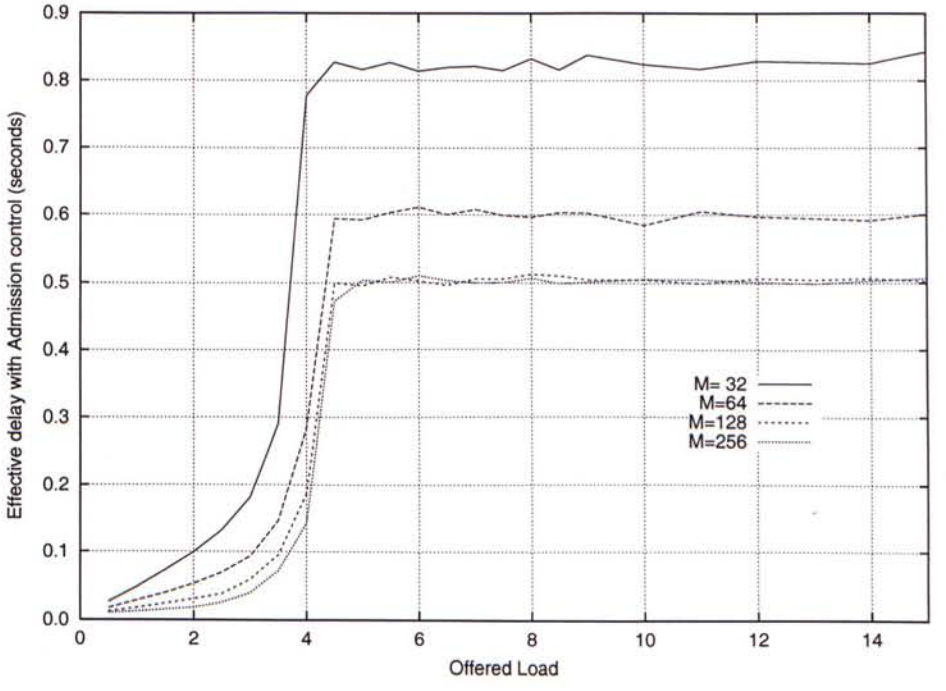


Figure 3.15: Mean random access delay with stability control for different M.

to the time of 0.5 seconds) in our simulation.

## 3.4 Multi-class Model

We now construct the multi-class model then find the throughput and verify the stability with a modified stability control algorithm as shown in figure 3.16. In addition to the previous assumptions, an extra assumption is needed in multi-class model: We assume bursts of different classes and all the retransmitted bursts use different midambles. Therefore, Base Station can classify the types of received bursts hence $\widehat{A^i}(u)$ and $\widehat{R}(u)$ can be measured. To illustrate the model, we use an example with only two classes of traffic (HI and LOW prioirty bursts), and these bursts are completely independent. Note that this multi-class

Table 3.5: A comparison of expected effective throughput and the effective throughput with sinusoidal arrival model.

| $\gamma$ | $h(f(t))$ | Expected Effective Throughput | Effective Throughput | | |
|---|---|---|---|---|---|
| | | | $T = 1$ min | $T = 5$ mins | $T = 15$ mins |
| 6.7 | 5.70 | 4.30 | 4.30 | 4.29 | 4.30 |
| 6.2 | 6.14 | 4.31 | 4.28 | 4.29 | 4.30 |
| 5.7 | 5.38 | 4.33 | 4.31 | 4.29 | 4.30 |
| 5.2 | 4.76 | 4.30 | 4.30 | 4.28 | 4.29 |
| 4.7 | 4.70 | 4.30 | 4.17 | 4.15 | 4.14 |
| 4.2 | 4.20 | 4.20 | 3.90 | 3.91 | 3.92 |
| 4.0 | 4.00 | 4.00 | 3.81 | 3.82 | 3.81 |
| 3.0 | 3.00 | 3.00 | 2.97 | 3.00 | 3.00 |
| 2.0 | 2.00 | 2.00 | 1.98 | 2.00 | 2.00 |
| 1.0 | 1.00 | 1.00 | 1.00 | 0.96 | 0.95 |

model can in fact incoroprate more than 2 classes of bursts. The HI priority bursts carry the control messages, such as location update messages, call-initial-messages and emergency calls. The LOW priority bursts carry the small size packets, the requests of CPCH, or the requests of DCH. Since the control message are very important to the system and they should be transmitted whenever a UE wants with as few retransmissions as possible. Thus, our algorithm should first assign the capacity to these bursts. On the other hand, the LOW priority bursts are most likely being blocked when the random access channel load is high. The blocking probabilities for HI and LOW classes bursts are also broadcast on the BCCH before each random access slots.

We find the system throughput and stability by computer simulation. The simulation model and parameters are as same as that in single class model. First, we assume that the arrival rate of the HI and LOW priority bursts are

Table 3.6: Effective throughput versus different values of $u$ for the sinusoidal arrival model.

| $\gamma$ | $h(f(t))$ | $u=1$ | $u=2$ | $u=5$ | $u=10$ | $u=100$ | $u=200$ | $u=1000$ |
|---|---|---|---|---|---|---|---|---|
| 6.7 | 5.7 | N/A | 3.63 | 4.06 | 4.18 | 4.30 | 4.28 | 4.12 |
| 6.2 | 6.14 | N/A | 3.68 | 4.11 | 4.20 | 4.28 | 4.27 | 4.24 |
| 5.7 | 5.38 | 3.56 | 3.86 | 4.15 | 4.22 | 4.31 | 4.28 | 4.14 |
| 5.2 | 4.76 | 3.75 | 3.93 | 4.09 | 4.17 | 4.31 | 4.29 | 4.21 |
| 4.7 | 4.7 | 3.79 | 3.92 | 4.06 | 4.12 | 4.17 | 4.17 | 4.14 |
| 4.0 | 4.0 | 3.56 | 3.68 | 3.74 | 3.81 | 3.81 | 3.82 | 3.80 |

Step 1. $G = G^* - \widehat{R}(u)$

Step 2. for $i = 1$ to $k$ do *[k classes of bursts]*

{

if $G \leq 0$ then { $P_a^i = P_a^{i+1} = \cdots = P_a^k = 0$; goto Step 3;};

if $G \geq \widehat{A^i}(u)$ then $P_a^i = 0$ ; else $P_a^i = \frac{G}{\widehat{A^i}(u)}$;

$G = G - \widehat{A^i}(u)$;

}

Step 3. Broadcast the access probabilities $P_a^i$, $i = 1, ..., k$.

[END]

Figure 3.16: The Random Access Channel Stability Control Algorithm for Multi-Class Model.

Possion Processes of rate 1 and $\gamma$ (bursts/access slot), respectively. Figure 3.17 shows the effective throughput for both HI and LOW priorities bursts. With stability control, the system is stable althought the total offered load is high. The effective delays for the bursts are shown in figure 3.18. From these results, we can see that our stability control algorithm works perfectly for multiclass random access bursts.

Second, sinusoidal arrival model is used for the generation of LOW priority

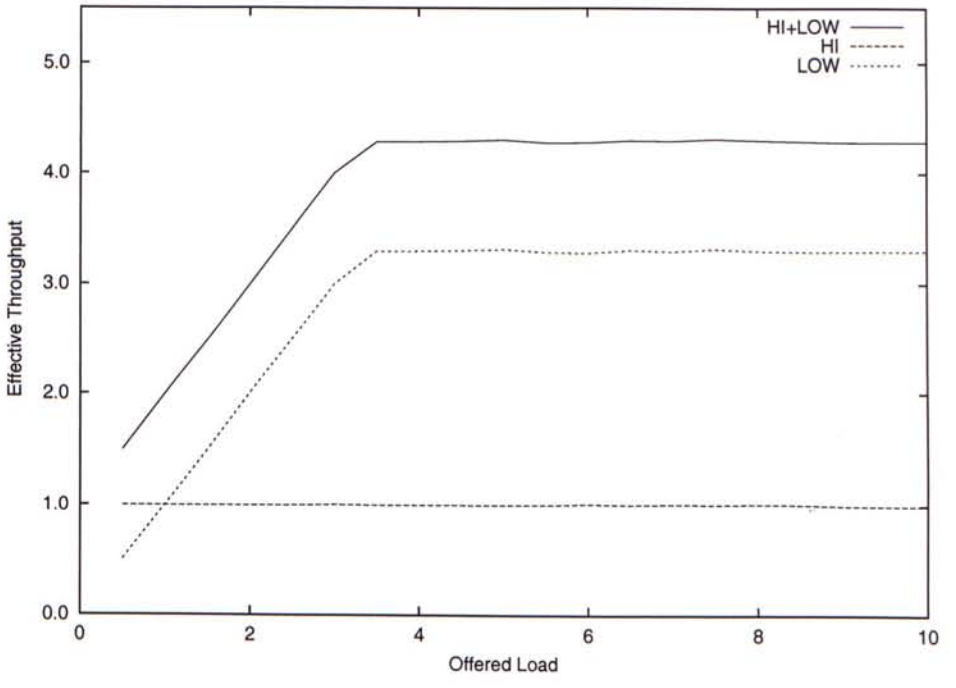


Figure 3.17: Effective throughput of two classes of bursts with stability control.

random access bursts. The HI priority random access bursts are still generated with a Poission process of a rate 1 (bursts/slot). Table 3.7 lists the throughputs for two classes of bursts with the duration $T$ as a parameter. From the results we know that the system is stable under the control of the stability control algorithm. Thus, our stablility control algorithm also works well under the mulit-class case.

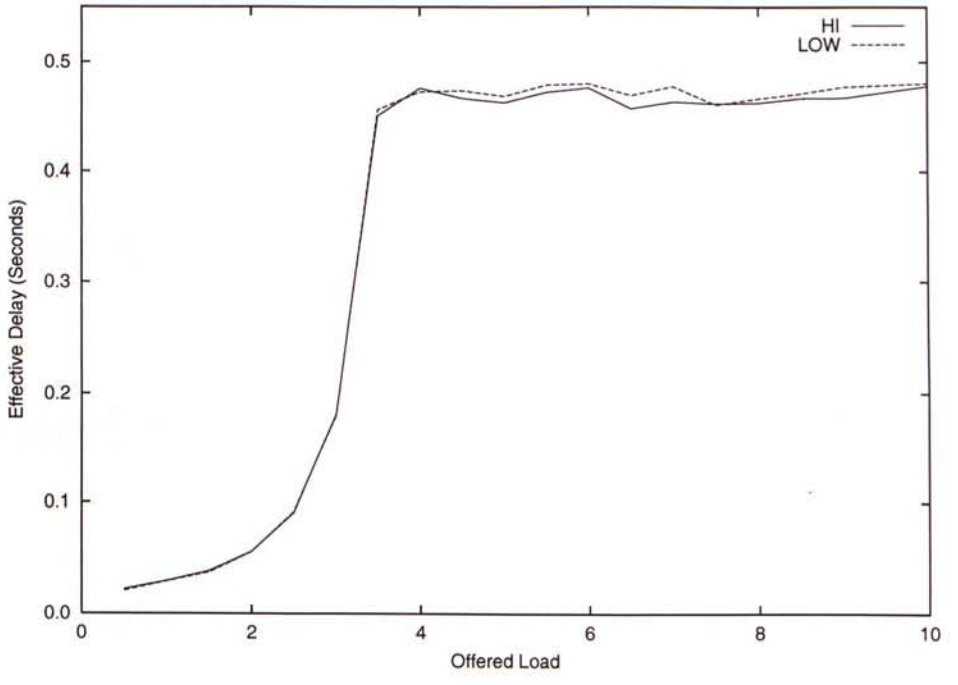


Figure 3.18: Mean Random Access delays of two classes of bursts with stability control.

Table 3.7: A comparison of expected effective throughput and the effective throughput with sinusoidal arrival model in multi-class case.

| $\gamma$ | $h(f(t))$ | Expected Effective Throughput | | Effective Throughput | | | | | |
|---|---|---|---|---|---|---|---|---|---|
| | | | | $T = 1$ min | | $T = 5$ mins | | $T = 15$ mins | |
| | | HI | LOW | HI | LOW | HI | LOW | HI | LOW |
| 5.7 | 5.38 | 1.00 | 3.30 | 0.98 | 3.30 | 1.00 | 3.30 | 1.00 | 3.30 |
| 5.2 | 4.76 | 1.00 | 3.30 | 0.99 | 3.30 | 0.99 | 3.30 | 1.00 | 3.30 |
| 4.7 | 4.70 | 1.00 | 3.30 | 1.00 | 3.28 | 1.00 | 3.29 | 1.00 | 3.30 |
| 4.2 | 4.20 | 1.00 | 3.29 | 0.98 | 3.29 | 0.99 | 3.29 | 1.00 | 3.29 |
| 3.7 | 3.70 | 1.00 | 3.14 | 0.98 | 3.14 | 1.00 | 3.14 | 1.00 | 3.14 |
| 3.2 | 3.20 | 1.00 | 2.92 | 1.00 | 2.91 | 1.00 | 2.92 | 1.00 | 2.92 |
| 3.0 | 3.00 | 1.00 | 2.81 | 1.00 | 2.81 | 1.00 | 2.80 | 1.00 | 2.81 |
| 2.0 | 2.00 | 1.00 | 2.00 | 0.99 | 2.00 | 1.00 | 1.99 | 1.00 | 2.00 |
| 1.0 | 1.00 | 1.00 | 1.00 | 0.99 | 1.00 | 1.00 | 0.97 | 1.00 | 0.96 |

# Chapter 4

# Conclusions and Topics for Future Study

## 4.1 Thesis Conclusions

In Chapter 1, we first introduced some 2.5G systems that can offer medium-data rate. We also showed the possible evolution paths for these systems toward 3G. We described the physical layer of the UTRA system.

In Chapter 2, we purposed a Spreading Factor Optimization Algorithm for FDD downlink dedicated channels. This algorithm can maintain the average bandwidth wastage being less than 10%. It changes the spreading factor frame by frame and assigns maximum number of dedicated channels for each request.

In Chapter 3, we studied the random access in the TD/CDMA system of IMT-2000. We found the maximum system throughput by mathematical analysis and computer simulations. If the arrival rate of the random access bursts is too high, i.e. over the maximum system capacity, the number of collided

bursts will be increase and they should be retransmitted some time later. This could bring the system into an unstable state. Therefore, we derive a Stability Control Algorithm; it can block some random access burst arrivals and maintain the system in a stable state with near maximum throughput when the random access burst arrival rate is very high. We use the blocking probability and the random access burst arrival rate of previous access slots to estimate the random access burst arrival rate in the next coming random access slot. This algorithm is simple, fast and robust for multi-class random access bursts under the tests of both constant and sinusoidal arrival mode.

## 4.2 Future Work

There are undoubtedly still interesting problems to be solved for the 3G systems, especially in the resource allocation problems. We now highlight some important issues and possible extensions of this research:

Since the 3G physical layer is a new standard, there are many problems to be solved.

### 4.2.1 Downlink and Uplink resource allocation in TDD

The boundary between uplink and downlink time slots of a TDD frame is movable frame by frame. Finding an algorithm to balancing the uplink and downlink traffic by adjusting this boundary is needed. Moreover, since the random access characteristic is unpredictable in the uplink, if too many random access bursts are transmitted in a particular time slot of a frame in Cell A, the power of these

bursts will interfere the downlink bursts in the same time slot of Cell A's surrounding cells. If we take this into account, the algorithm will be more complex. It is interesting to define a model and find an algorithm for this problem.

### 4.2.2 Resource Unit Packing in TDD

In UTRA TDD system, a Resource Unit (RU) is defined as the association of one-code, one time slot and one frequency. There are a total of $8 \times 15 = 120$RUs in each frame. Different services request different number of RUs in each frame. If we assign these requests with RUs arbitrarily, some wastage of RUs and a poor utilization will result. Thus, we should find a algorithm to fully pack the requesting RUs to the frame.

### 4.2.3 Other Topics

1. We also need Admission Control and Resource Allocation algorithms for different services to meet different QoS requirements.

2. On the infrastructure site, the backbone is based on a IP network. Packets are transferred between MSCs, BSs, and UEs. Traffic Engineering problems for this network are also interesting.

# Bibliography

[1] http://www.3gpp.org, The 3rd Generation Partnership Project, it is a Global specifications for GSM/MAP network evolution to 3G and the UTRA RTT.

[2] IEEE P802.11, Draft Standard of Wireless Lan, 9 May 1997, p.95-96

[3] 3rd Generation Partnership Project; Technical Specification Group Radio Access Network; MAC protocol specification 3G TS 25.321 V3.3.0(2000-03)

[4] 3rd Generation Partnership Project; Technical Specification Group Radio Access Network; Physical channels and mapping of transport channels onto physical channels (FDD) 3G TS 25.211 V.3.2.0(2000-03)

[5] D. Raychaudhri, "Performance Analysis of Random Access Packet-Switched Code Division Multiple Access Systems," IEEE Transactions of Communication, vol. COM-29, pp. 895-901, June 1981.

[6] Fredrik Ovesjo, Erik Dahlman, Tero Ojanpera, Antii Toskala, Anja Klein, "FRAMES MULTIPLE ACCESS MODE 2 - WIDEBAND CDMA", The 8th IEEE International Symposium on Volume: 1, 1997, Page(s): 42 -46 vol.1

[7] Peter W. de Graaf and James S. Lehnert, "Performance Comparison of a Slotted ALOHA DS/SSMA Network and a Multichannel Narrow-Band Slotted ALOHA Network", IEEE TRAN. on COMM, VOL. 46, NO.4, APRIL 1998

[8] W.Mohr, "UTRA FDD and TDD, a harmonized proposal for IMT-2000", International Conference on Communication Technology, ICCT'98 Ocb 22-24, 1998.

[9] TERO OJANPERA and RAMJEE PRASAD, "An Overview of Third-Generation Wireless Personal Communications: A Europe Perspective", IEEE Personal Communications, DEC 1998.

[10] htpp://www.mobilecdma.com/, Mobile CDMA

[11] http://www.gsmdata.com/, GSM Data Knowledge Site

[12] http://list.etsi.org/, List archives at LIST.ETSI.FR